Superconductivity and Magnetism in PRISTINE and in SULFUR DOPED AMORPHOUS CARBON (aC)

Israel Felner, Omri Wolf and Oded Millo

Racah Institute of Physics, The Hebrew University, Jerusalem, Israel

San Francisco 1 December 2014

Israel's Leading University

Outlines

1) Introduction to Superconductivity

2. Superconductivity in amorphous carbon (a-C)

3. Irreversible Magnetism in a-C and a-C+S

4. Summary

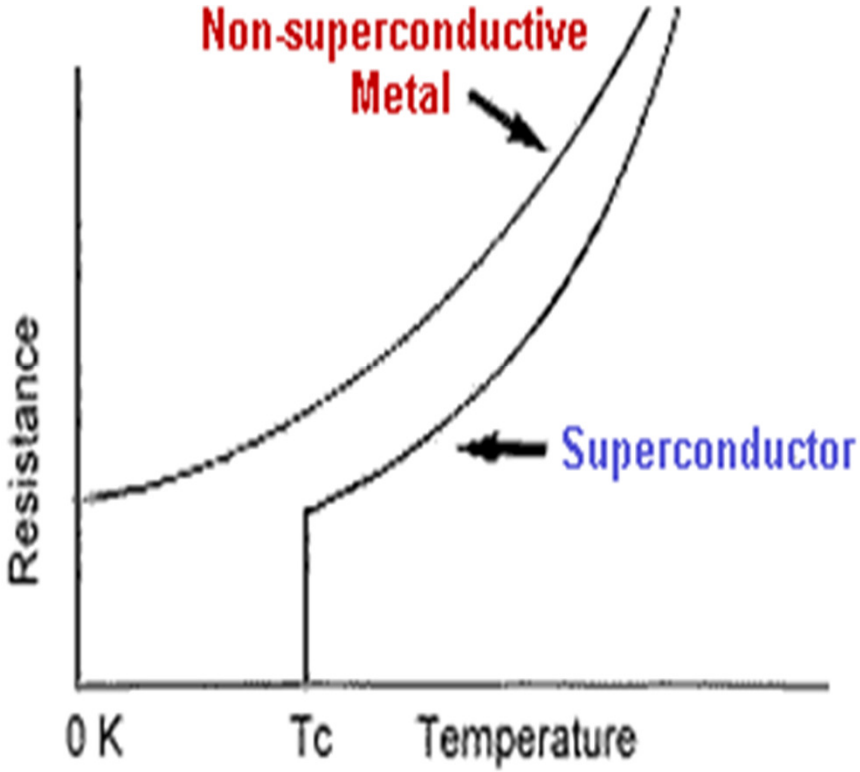
Review Article: Israel Felner, Materials Research Express 1 (2014) 016001

- **Superconductivity** discovered in Leiden on April 8, 1911 by Kamerlingh Onnes

1) Zero electrical resistance below T_C

2) Expulsion of magnetic field below T_C

Meissner effect (diamagnetism)



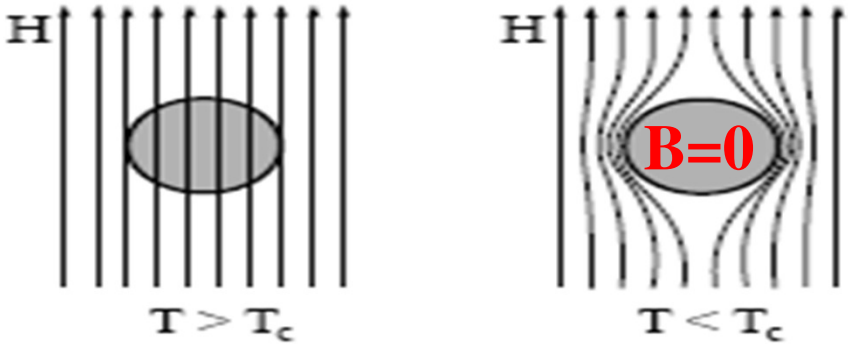
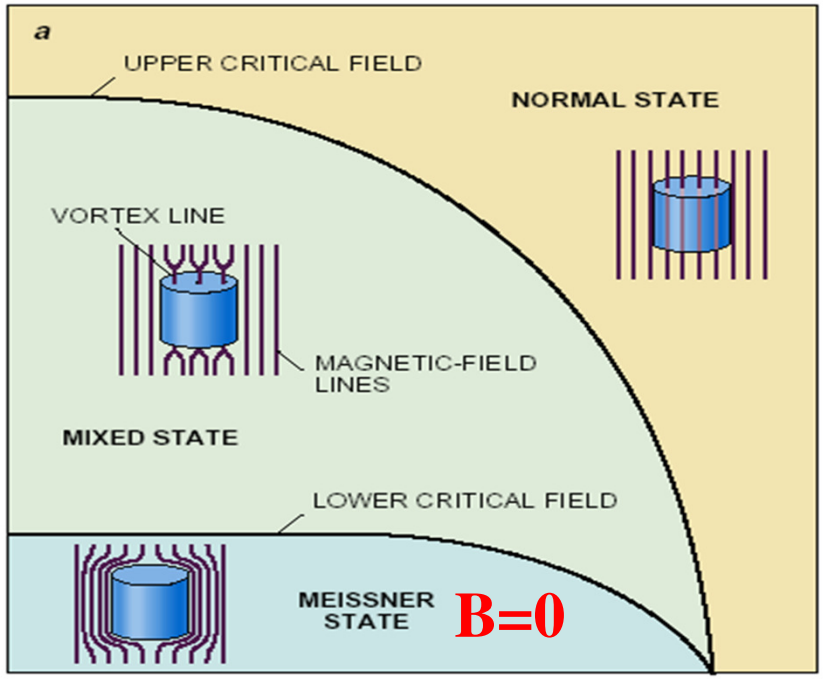


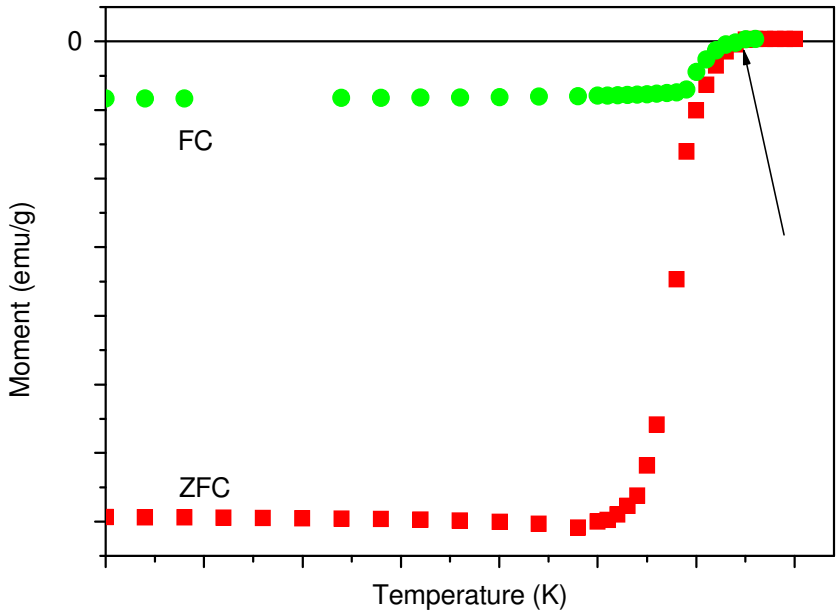
Figure 2.2. The Meissner effect: the expulsion of a weak, external magnetic field from the interior of a superconductor. The field is applied (a) at $T > T_c$, and (b) at $T < T_c$.

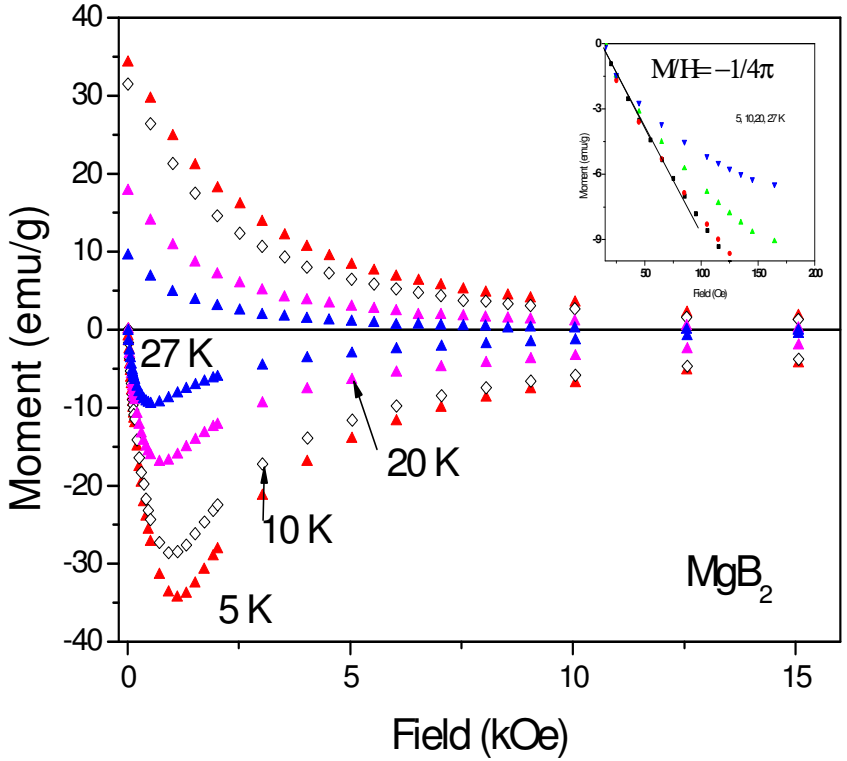
For **type II SC**, perfect diamagnetism inside the material (below H_{c1} B=0) $4\pi M+H=0$

$$M/H=-1/4\pi$$

$$H_c(T) \simeq H_c(0)[1-(T/T_c)^2],$$

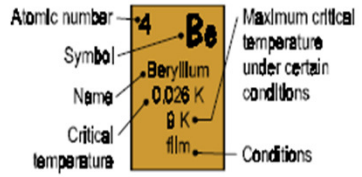






PERIODIC TABLE OF SUPERCONDUCTING ELEMENTS

from Yamashita T, Nakajima K, Chen J, Buzea C,
Superconductors - Scientific Basics and Engineering Applications
(Springer-Verlag, Heidelberg) 2002 to appear

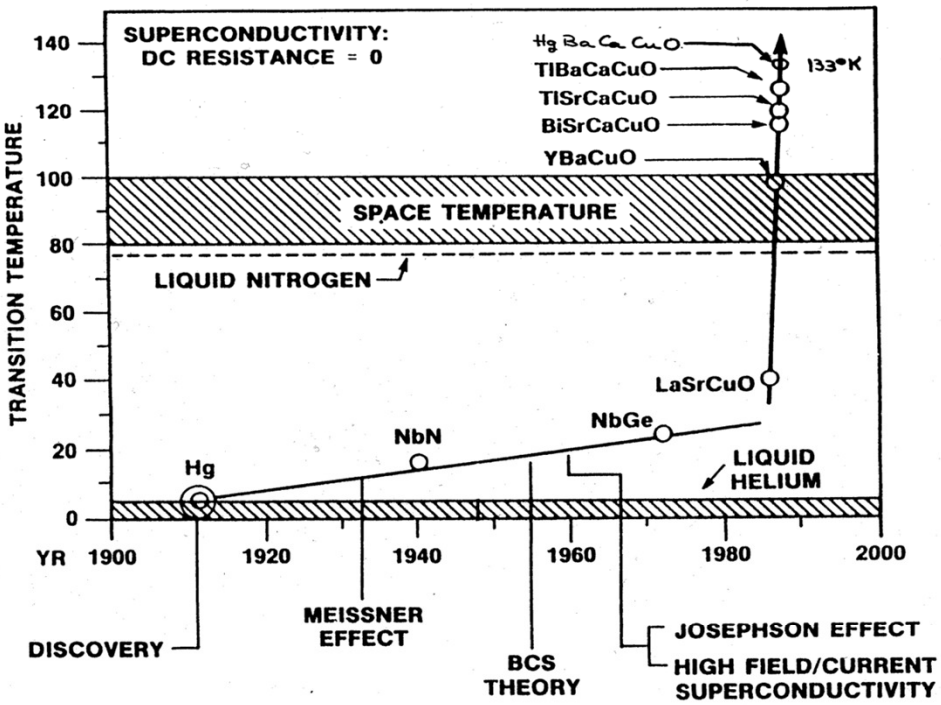


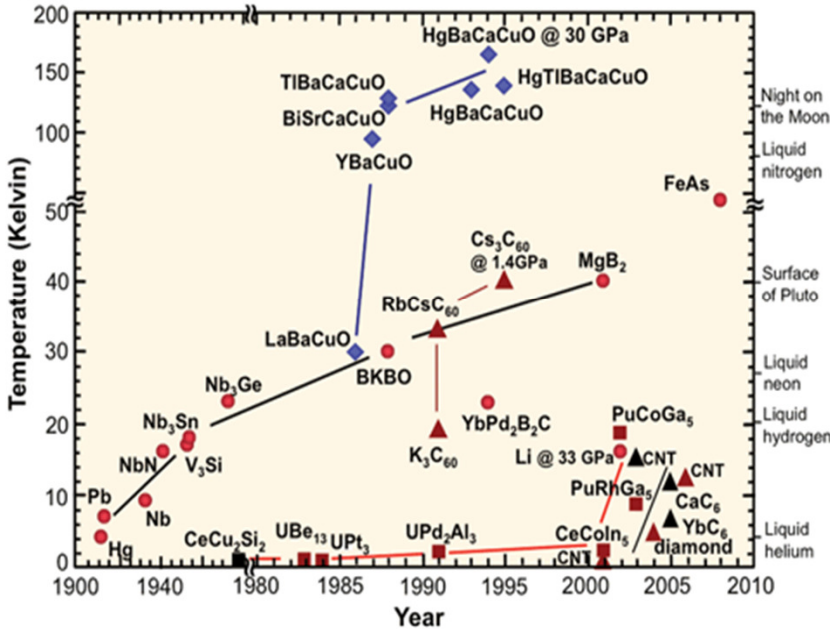
Superconducting element
Nonsuperconducting element
Superconducting element only under pressure or in film form

IA	IIA	IIIA	IVA	VA	VIA	VIIA	VIIIA		IB	IIB	IIIB	IVB	VB	VIB	VIIB	VIII
1 H Hydrogen																2 He Helium
3 Li Lithium 7 K 26 GPa	4 Be Beryllium 0.026 K 9 K film										5 B Boron 11.2 K 250 GPa	6 C Carbon 52 K charge doped	7 N Nitrogen	8 O Oxygen 0.6 K 120 GPa	9 F Fluorine	10 Ne Neon
11 Na Sodium	12 Mg Magnesium										13 Al Aluminum 1.17 K 3.6 K film	14 Si Silicon 8.5 K 12 GPa	15 P Phosphorus 5.6 K 17 GPa	16 S Sulfur 17 K 160 GPa	17 Cl Chlorine	18 Ar Argon
19 K Potassium	20 Ca Calcium 15 K 150 GPa	21 Sc Scandium 0.3 K 21 GPa	22 Ti Titanium 0.4 K	23 V Vanadium 5.4 K 17.2 K 120 GPa	24 Cr Chromium film	25 Mn Manganese film	26 Fe Iron 2 K 21 GPa	27 Co Cobalt	28 Ni Nickel	29 Cu Copper	30 Zn Zinc 0.85 K	31 Ga Gallium 7.9 K 8.4 K film	32 Ge Germanium 5.4 K 11.5 GPa	33 As Arsenic 2.7 K 24 GPa	34 Se Selenium 7 K 13 GPa	35 Br Bromine 1.4 K 150 GPa	36 Kr Krypton
37 Rb Rubidium	38 Sr Strontium 4 K 50 GPa	39 Y Yttrium 2.8 K 15 GPa	40 Zr Zirconium 0.6 K	41 Nb Niobium 9.25 K 9.7 K 4.5 GPa	42 Mo Molybdenum 0.92 K	43 Tc Technetium 8.2 K	44 Ru Ruthenium 0.5 K	45 Rh Rhodium 0.035 mK	46 Pd Palladium film/Imad	47 Ag Silver	48 Cd Cadmium 0.52 K	49 In Indium 3.4 K 4.2 K film	50 Sn Tin 3.7 K 4.7 K film	51 Sb Antimony 3.6 K 8.5 GPa	52 Te Tellurium 7.4 K 35 GPa	53 I Iodine 1.2 K 25 GPa	54 Xe Xenon
55 Cs Cesium 1.5 K 5 GPa	56 Ba Barium 5 K 15 GPa		72 Hf Hafnium 0.18 K	73 Ta Tantalum 4.4 K	74 W Tungsten 0.01 K 5.5 K film	75 Re Rhenium 1.7 K	76 Os Osmium 0.7 K	77 Ir Iridium 0.1 K	78 Pt Platinum	79 Au Gold	80 Hg Mercury 4.15 K	81 Tl Thallium 2.4 K	82 Pb Lead 7.2 K	83 Bi Bismuth 8.7 K 9 GPa	84 Po Polonium	85 At Astatine	86 Rn Radon
87 Fr Francium	88 Ra Radium																

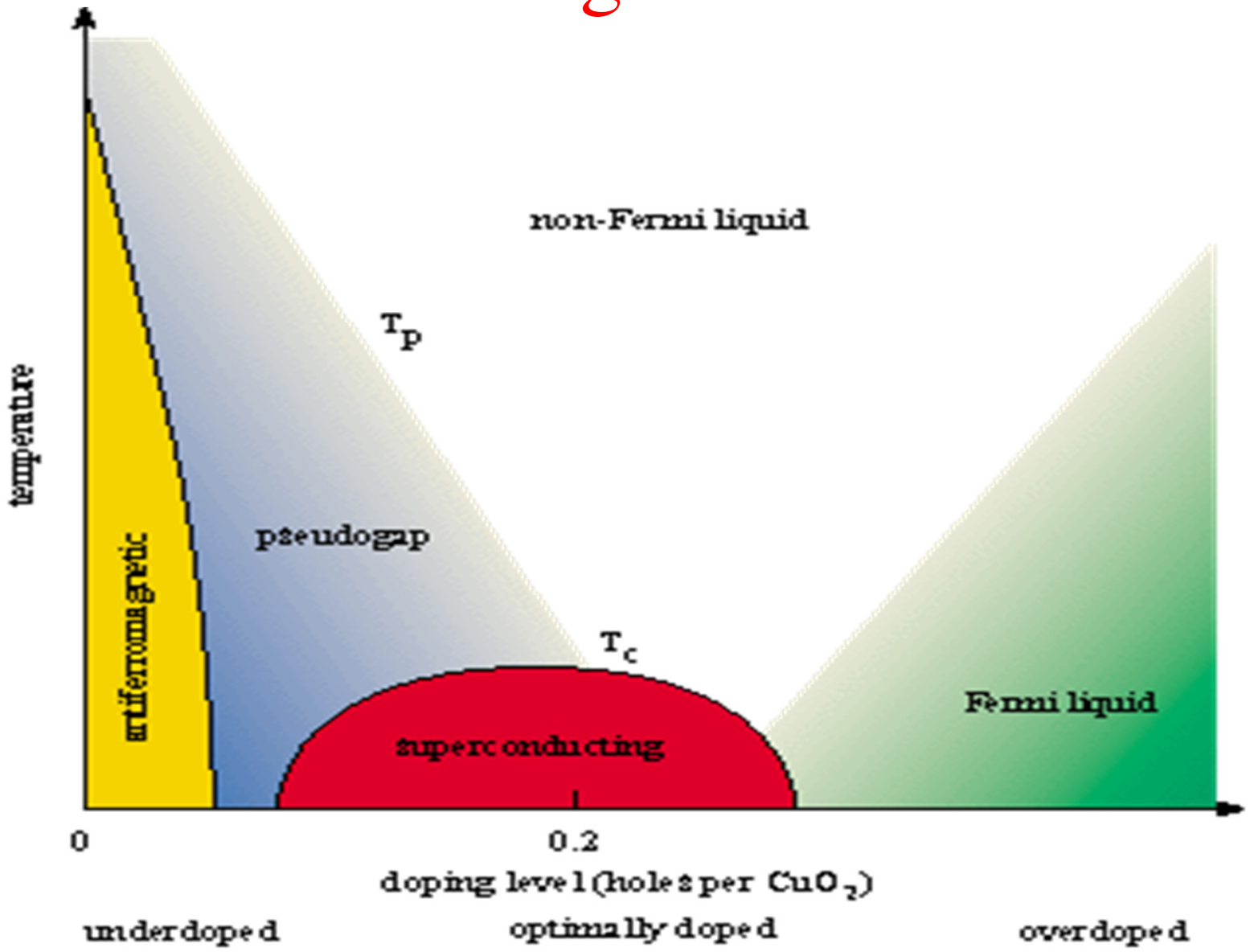
57 La Lanthanum 6 K 12 K 18 GPa	58 Ce Cerium 1.7 K film	59 Pr Praseodymium	60 Nd Neodymium	61 Pm Promethium	62 Sm Samarium	63 Eu Europium film	64 Gd Gadolinium	65 Tb Terbium	66 Dy Dysprosium	67 Ho Holmium	68 Er Erbium	69 Tm Thulium	70 Yb Ytterbium	71 Lu Lutetium 0.1 K
89 Ac Actinium	90 Th Thorium 1.4 K	91 Pa Protactinium 1.4 K	92 U Uranium 0.7 K 2.2 K 1 GPa	93 Np Neptunium	94 Pu Plutonium	95 Am Americium 1 K	96 Cm Curium	97 Bk Berkelium	98 Cf Californium	99 Es Einsteinium	100 Fm Fermium	101 Md Mendelevium	102 No Nobellium	103 Lr Lawrencium

High T_C superconductors

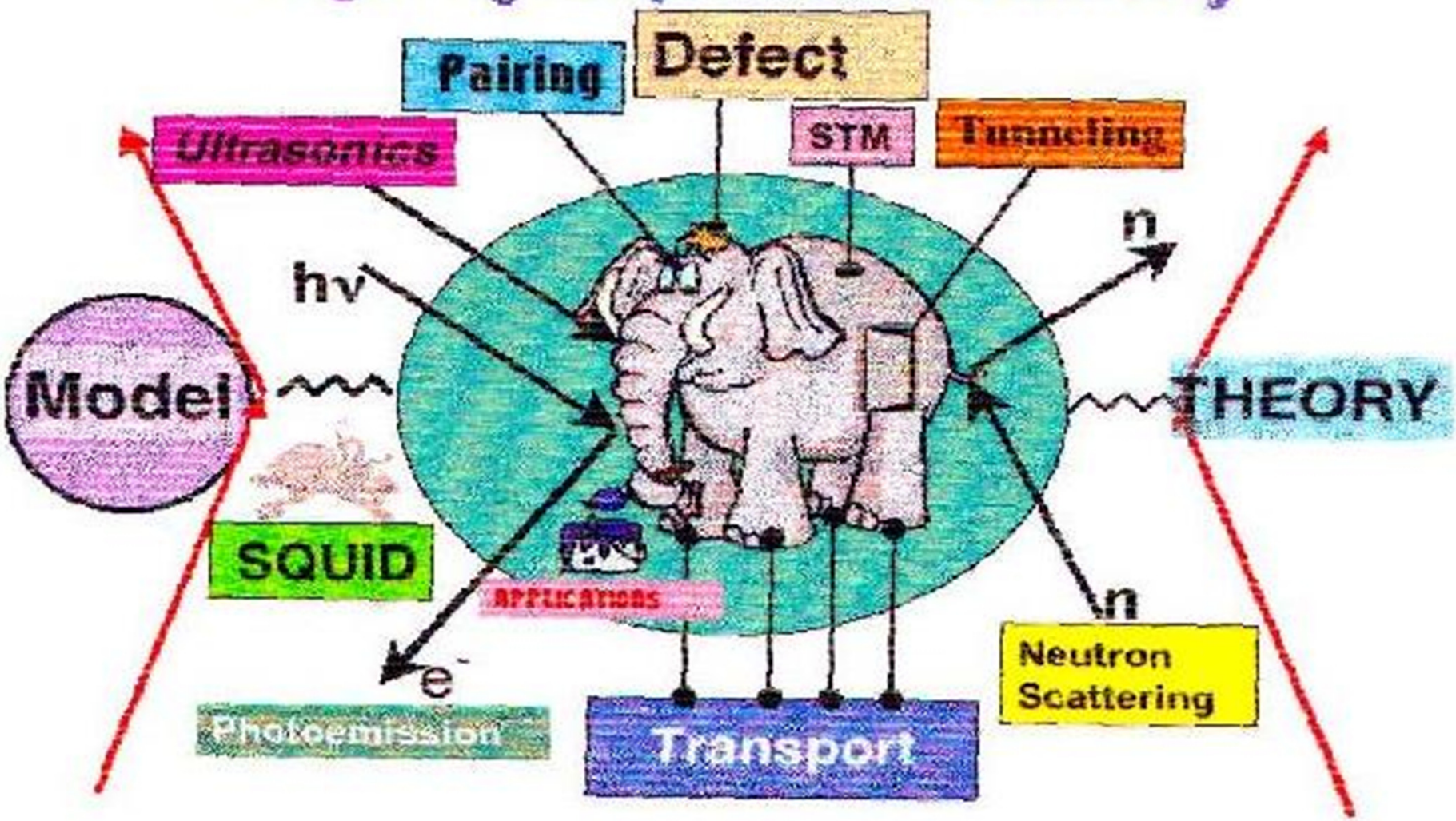




Phase diagram



High T_c Superconductivity



Commercial a-C powder manufactured by Fisher assigned as (C190-N) (1935) (for gas masks)

Inhomogeneity of the powder

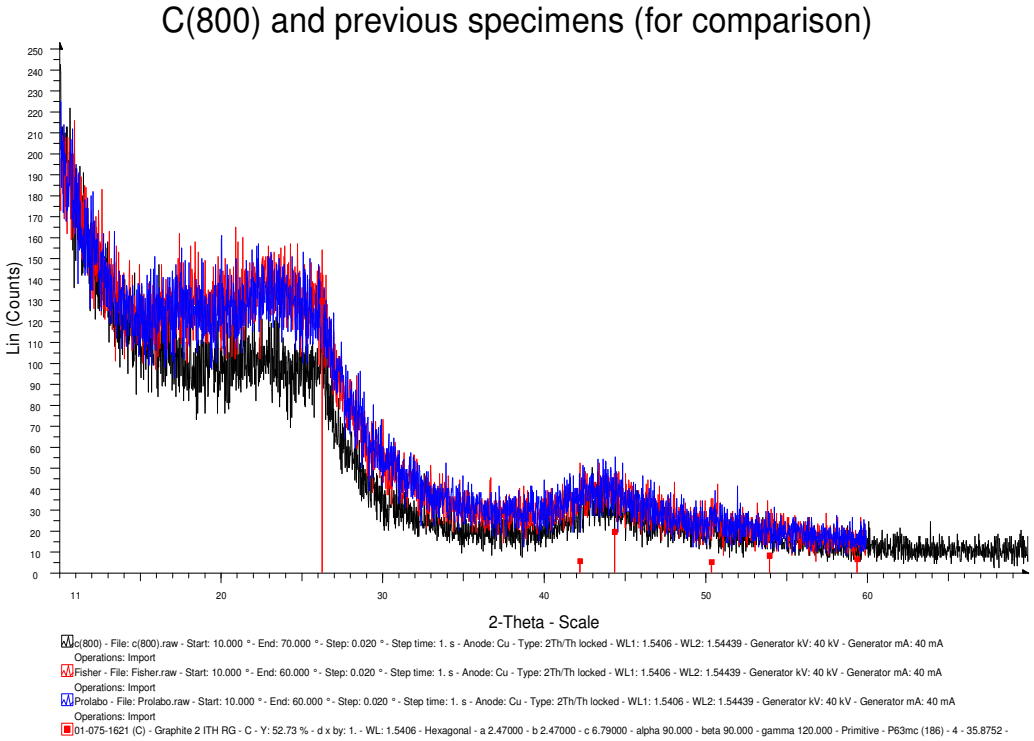
- **We measured 23 samples from the same container which are divided into *3 groups***

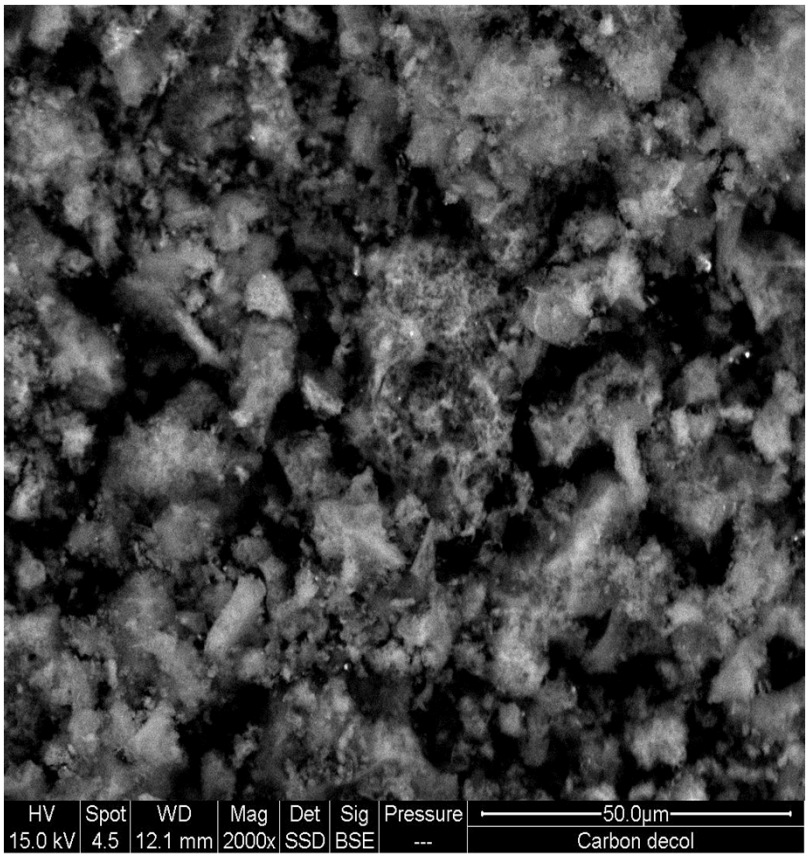
- **(1) In 16 samples no SC and no magnetism**

They exhibit the magnetic behavior of magnetite (Fe_3O_4)

- **(2) 3 samples show traces of SC up to 65 K!!!**
- **(3) 4 samples exhibit peculiar magnetic behavior**

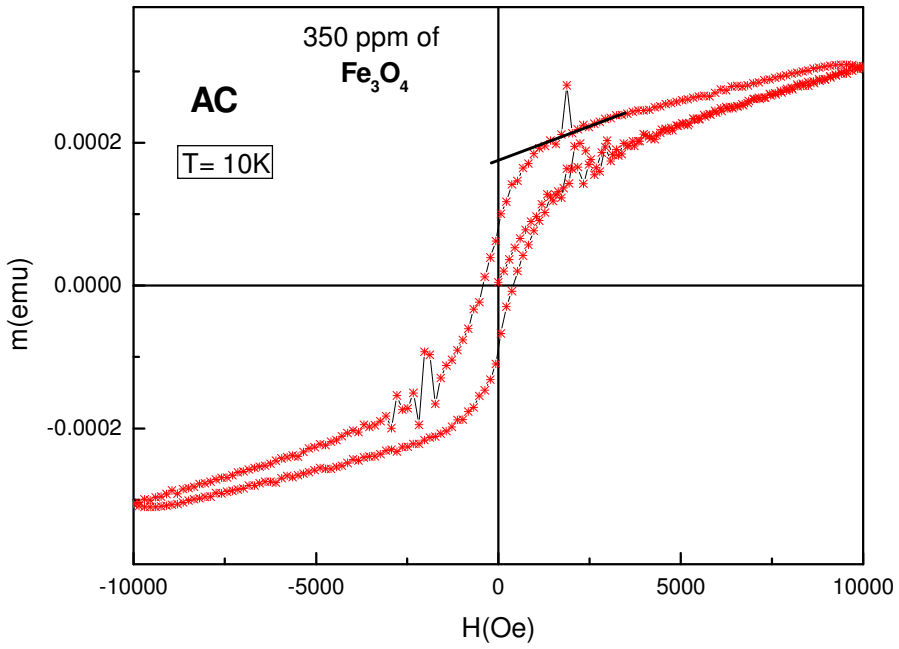
Commercial amorpous a-C powder

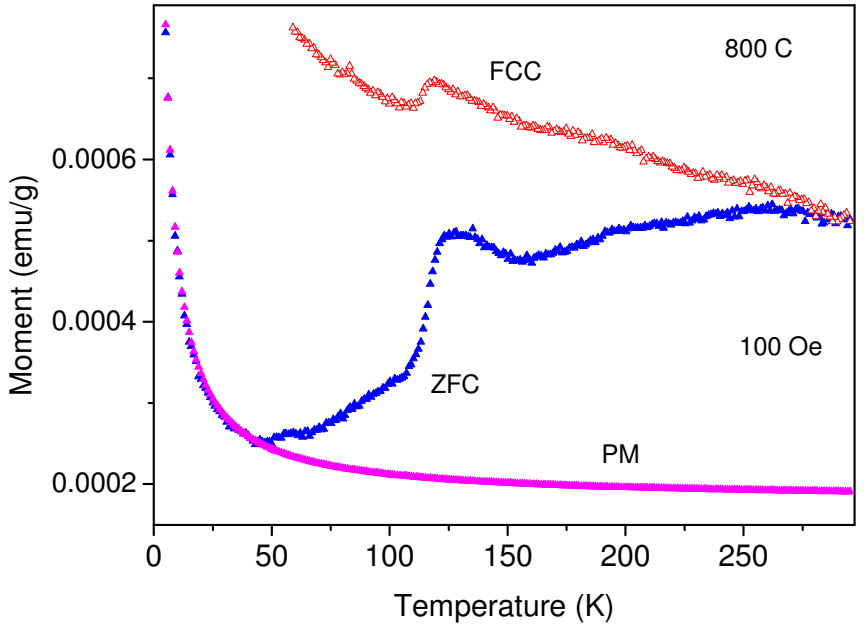




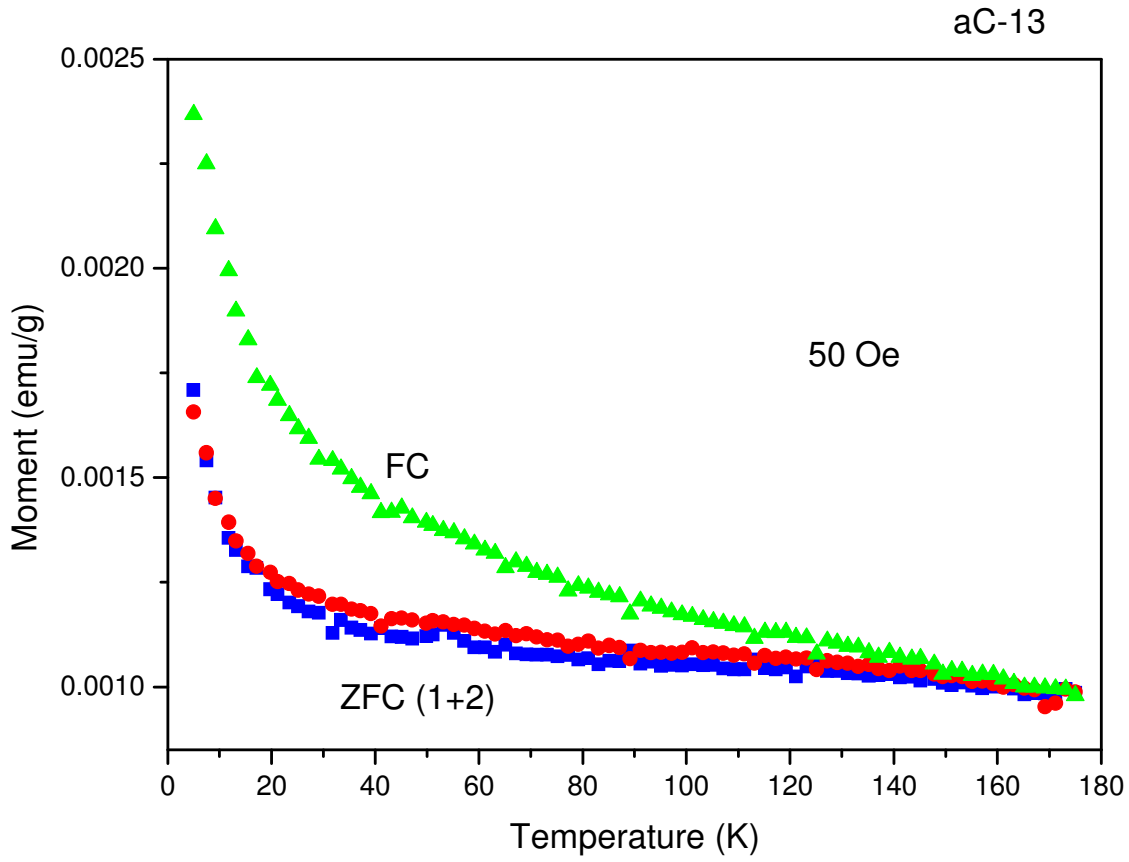
a-C sample heated at 800 C

Mossbauer studies show precisely the presence of 330-350 ppm of Fe_3O_4

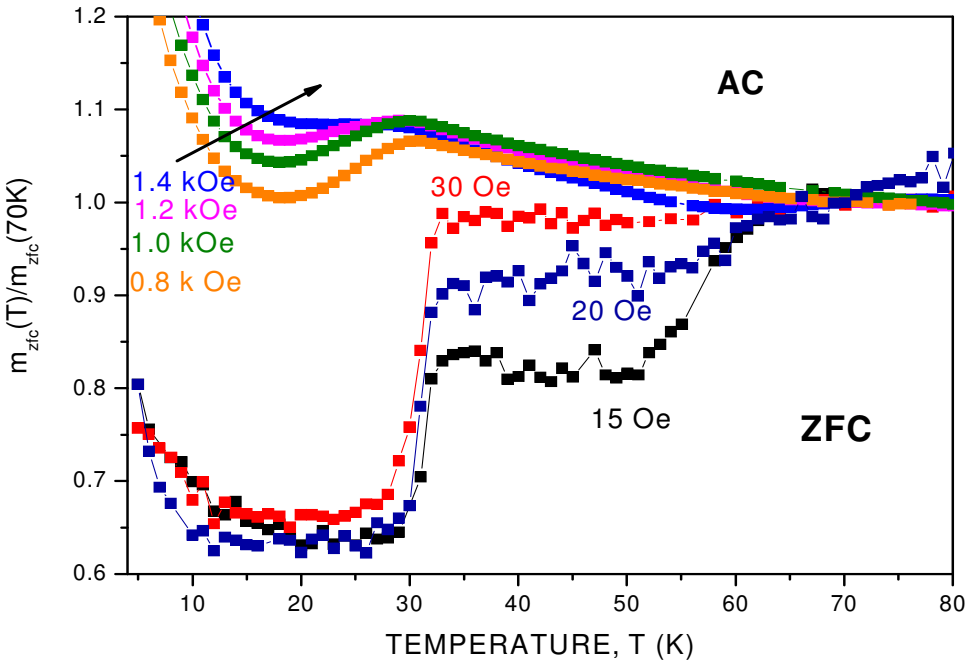


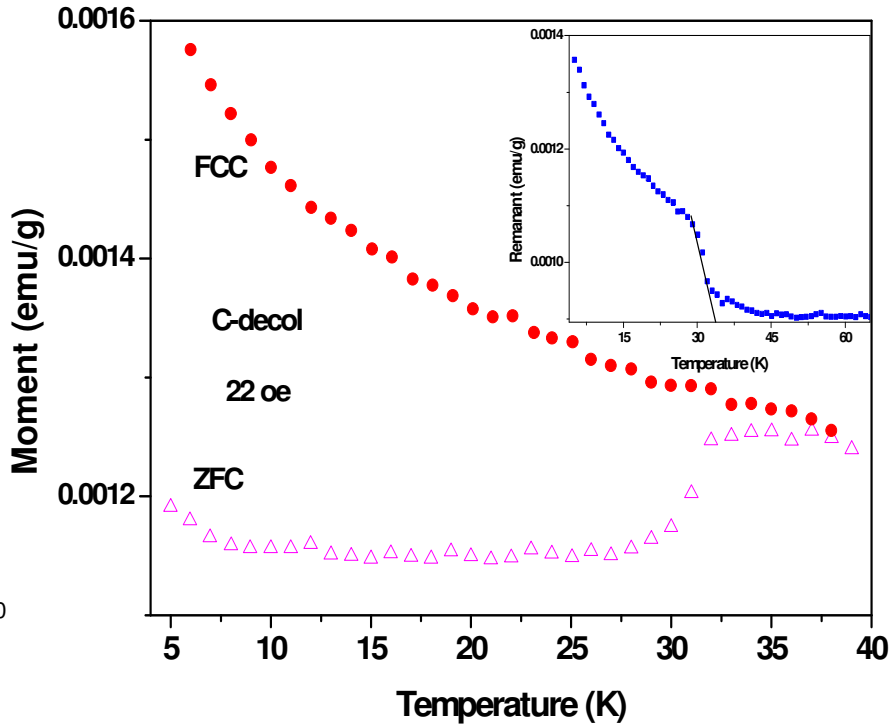


Group 1 (16 samples) Neither SC nor magnetic features



1) **Group 2** SC in Commercial a-C powder **sample No. 1**

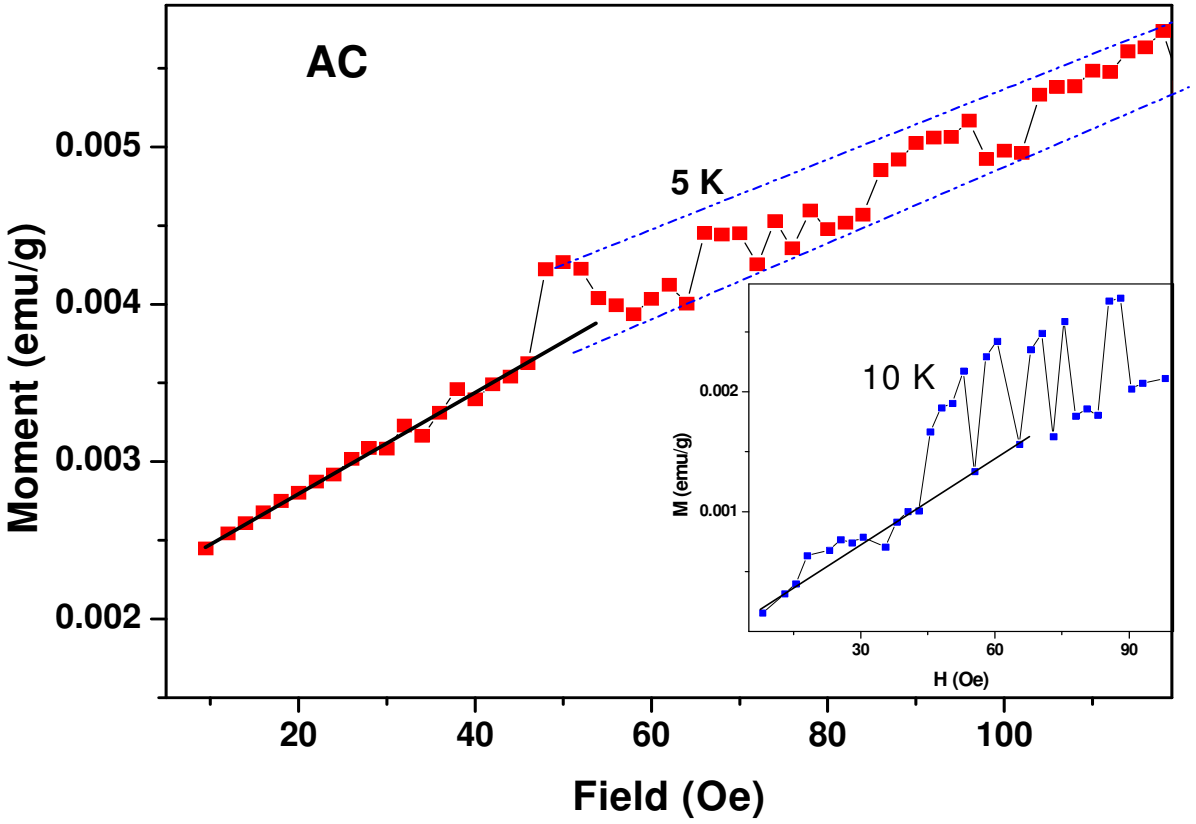




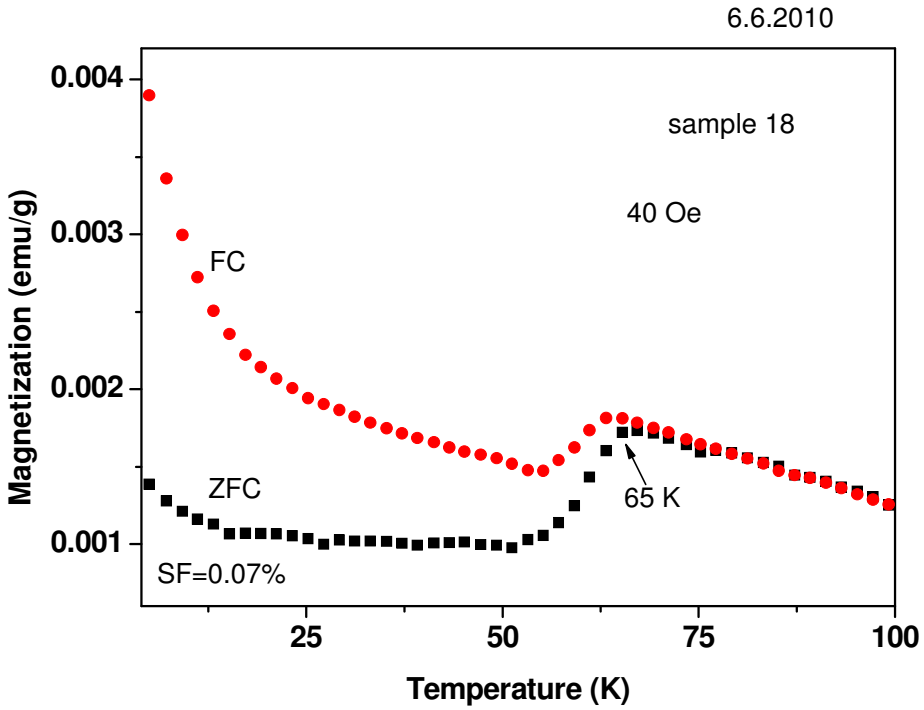
Two SC transitions at 32 and 63 K

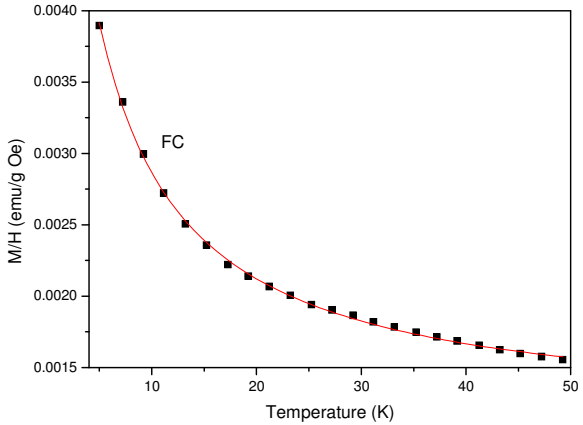
Shielding fraction (SF) 0.02% only

M(H) sample No. 1

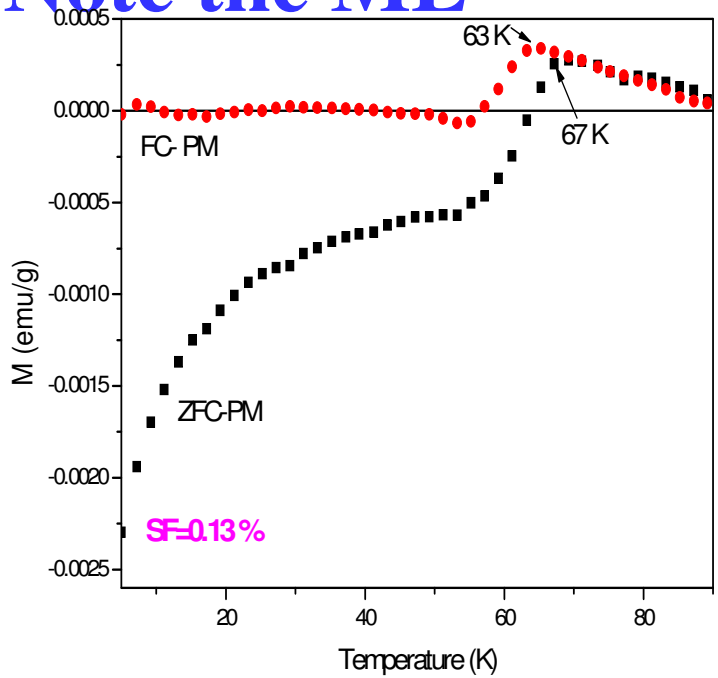


Commercial a-C (**sample No. 18**)



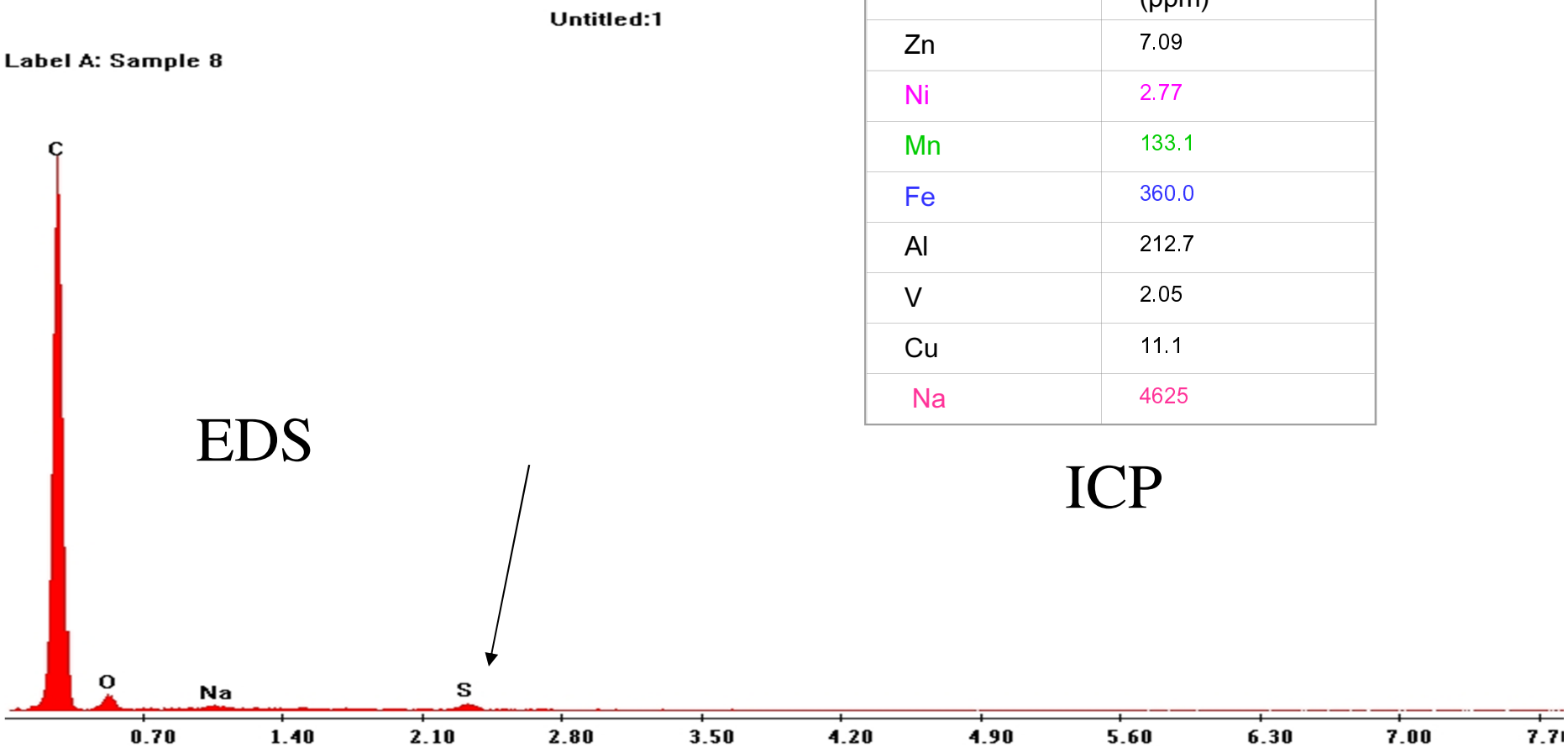


Note the ME



Superconductivity in carbon-based-materials (CBM)

CBM	T_C (K)	Year	
KC_8	0.15	Hannay et. al	1965
NaC_2	5	Belash et. al.	1987
CaC_6	11.5	Weller et. al.	2005
Cs_3C_{60}	38	Ganin et. al.	2008
HOPG (traces)	> 300	Esquinazi	2013



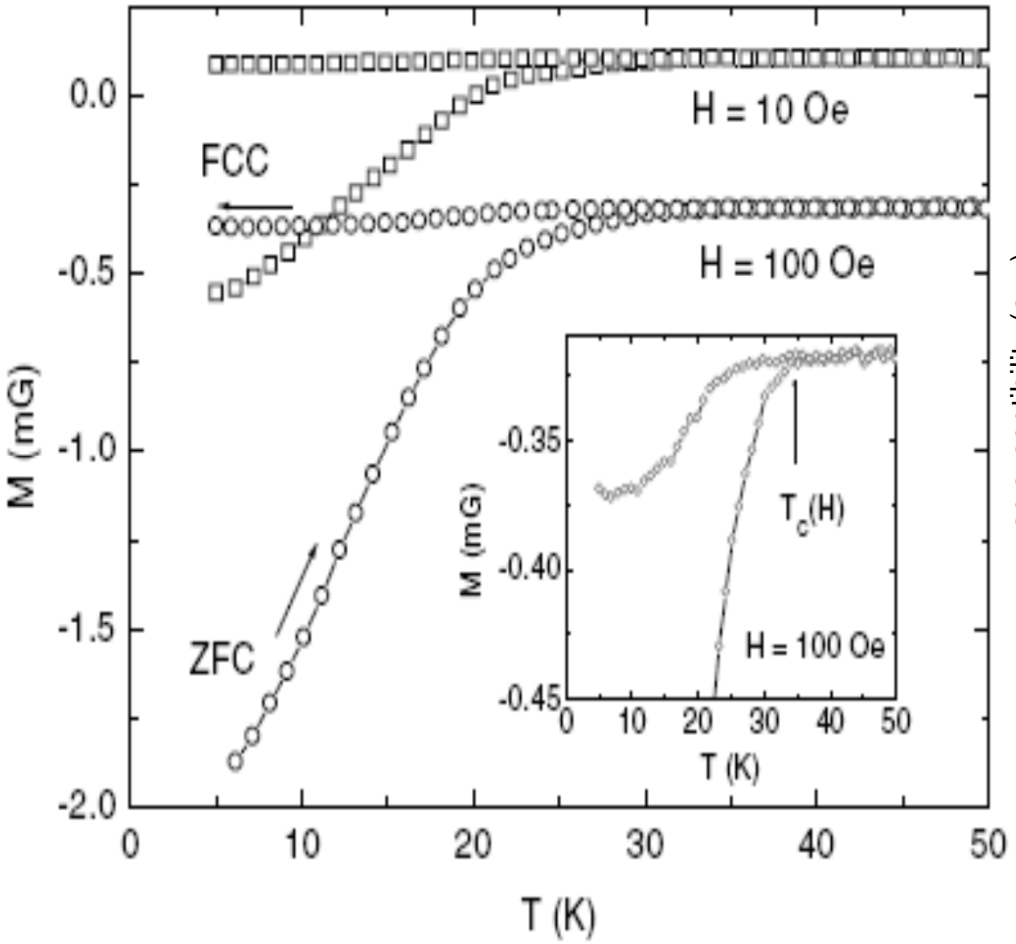
EDS

Element	Concentration (ppm)
Zn	7.09
Ni	2.77
Mn	133.1
Fe	360.0
Al	212.7
V	2.05
Cu	11.1
Na	4625

ICP

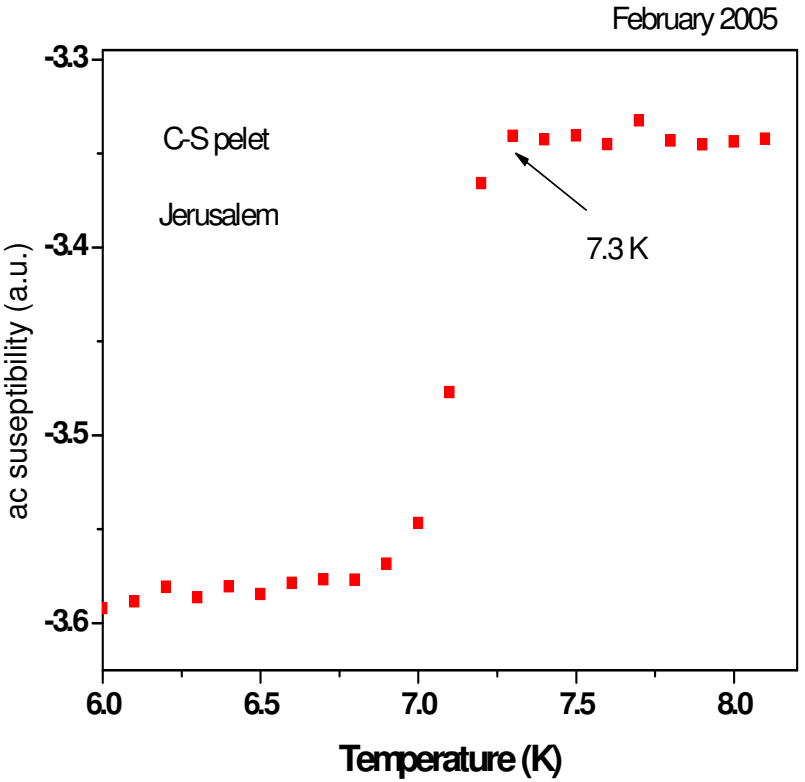
Highly pure graphite **powder +S**

T_c =35 K Shielding fraction ≈ 0.05 %



powder of ultra pure graphite

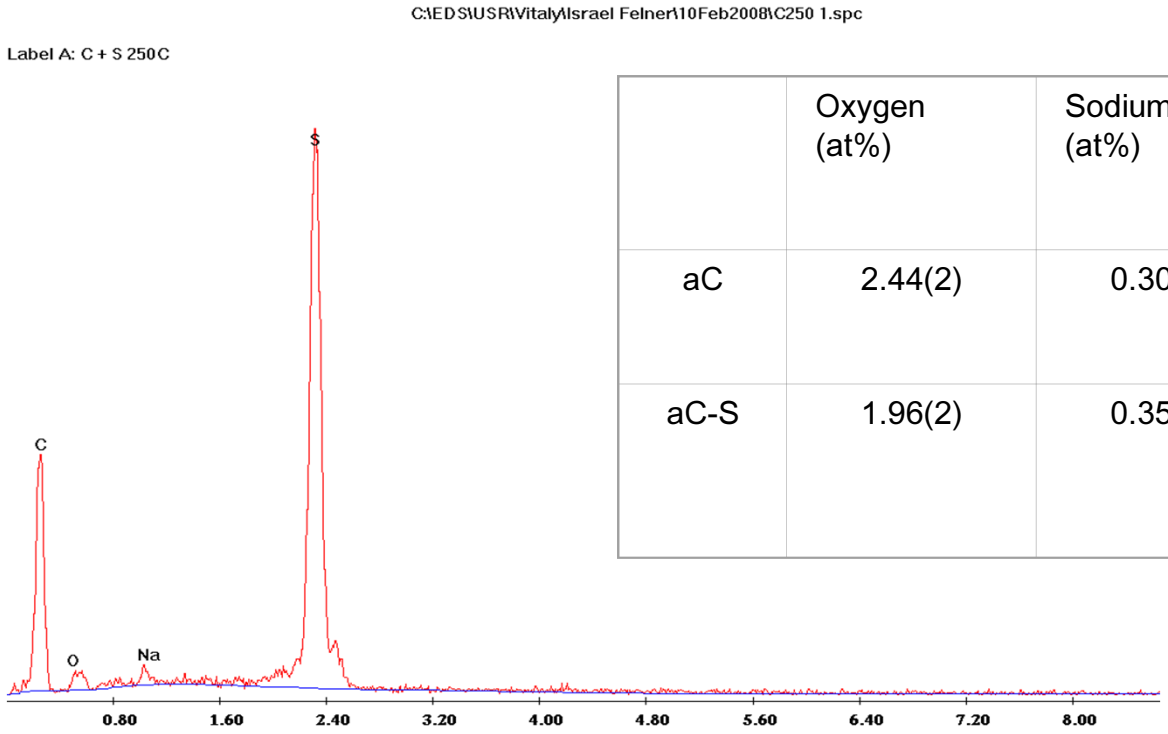
rod +S (Tc =7.3 K)



R. R. da Silva, et.al, Phys. Rev. Lett. **87**, 147001 (2001).

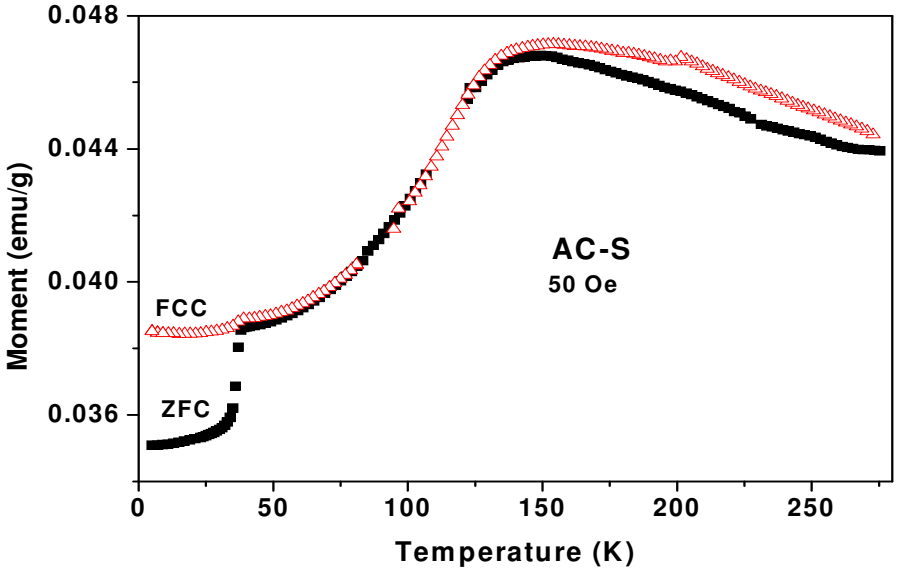
Motivation to use a-C+S

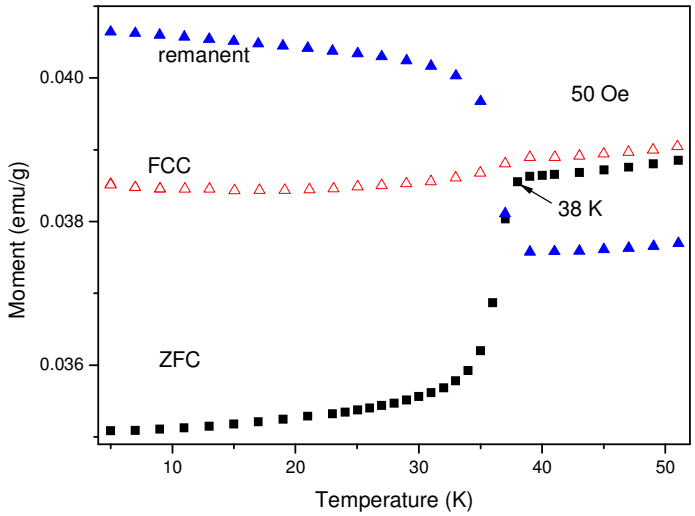
(2:1) heated at 250 C for 20h

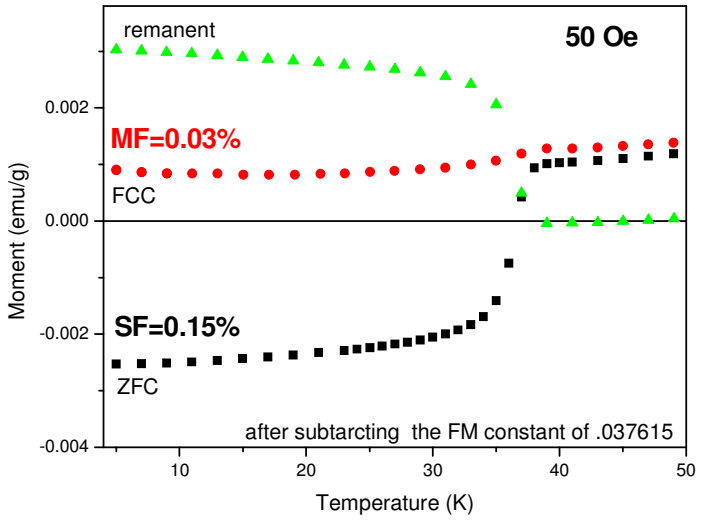


	Oxygen (at%)	Sodium (at%)	Sulfur (at%)
aC	2.44(2)	0.30(2)	0.21(2)
aC-S	1.96(2)	0.35(2)	10.3(1)

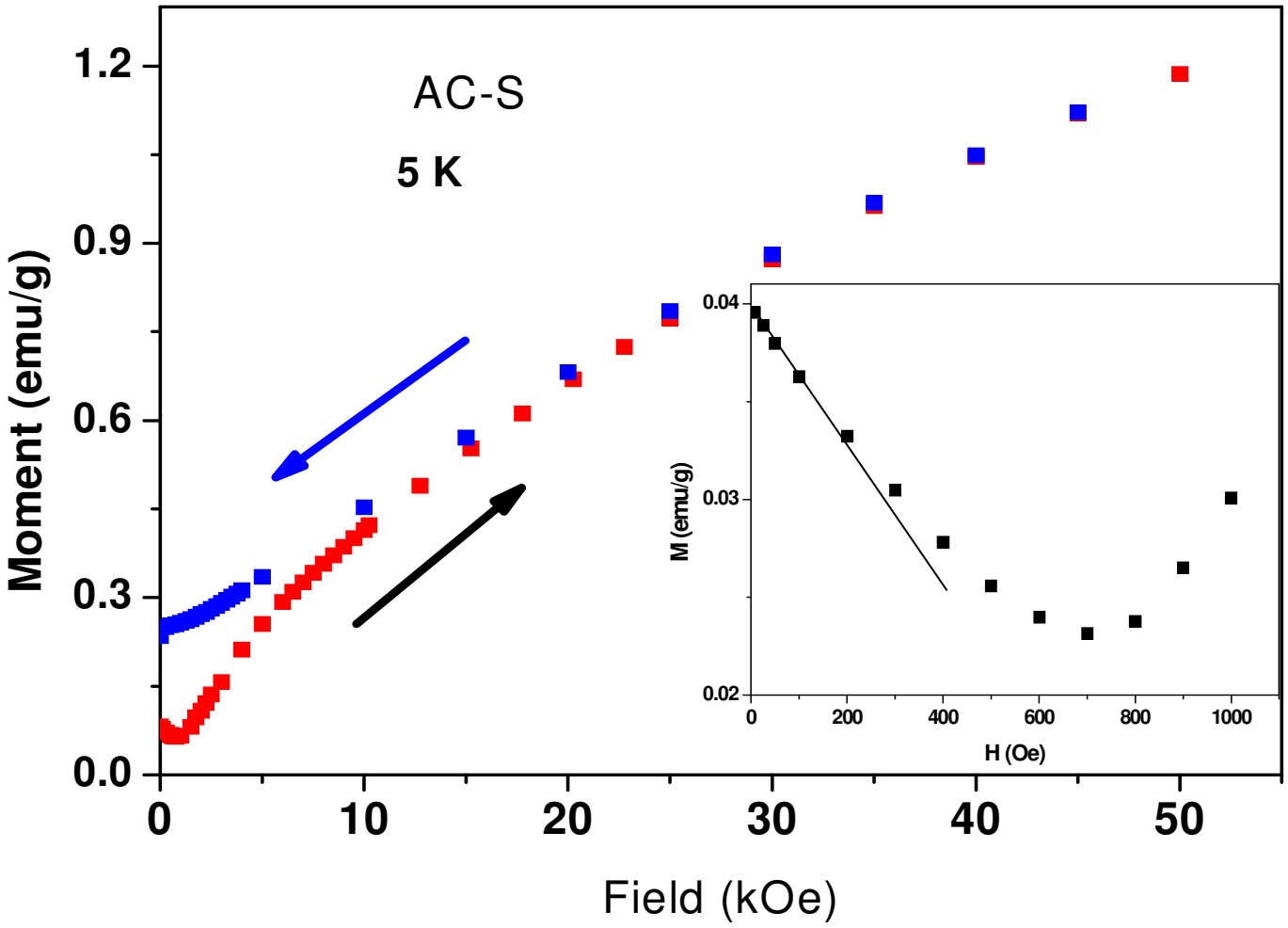
aC+S heated at 250 C



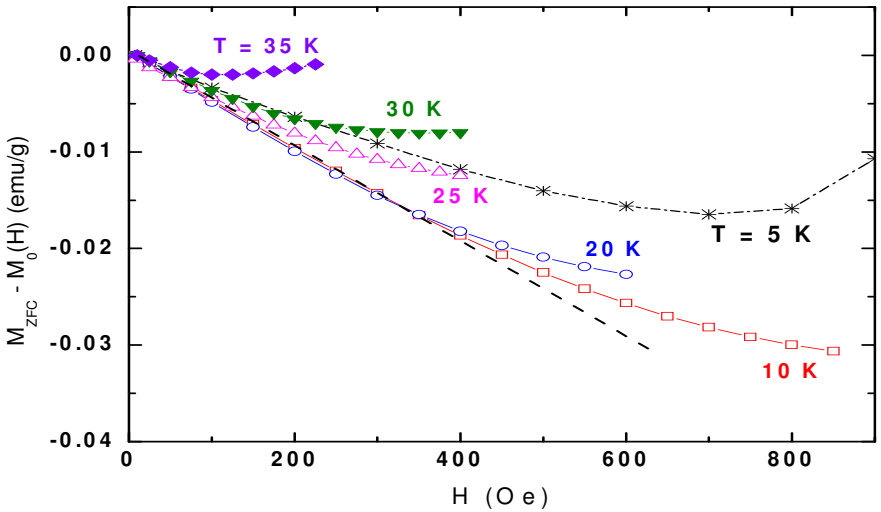


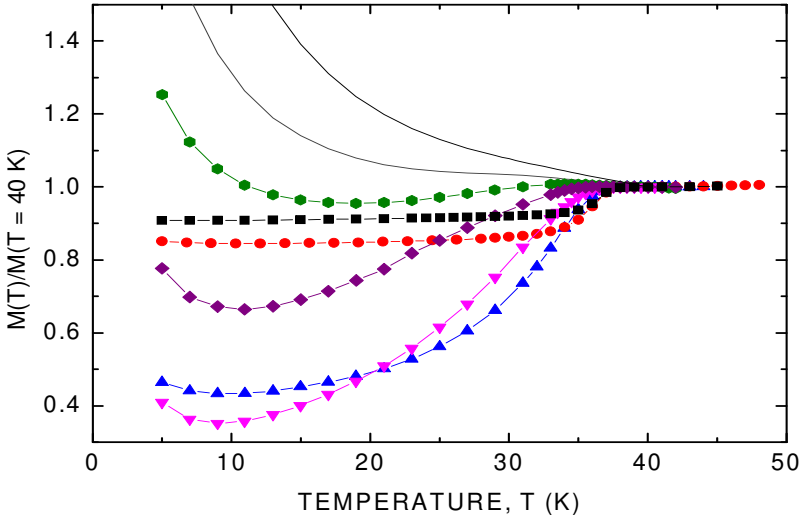


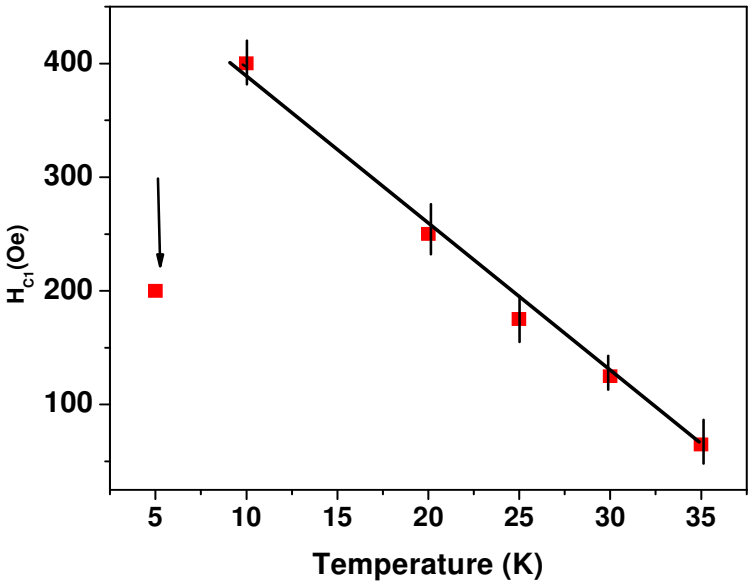
M(H)

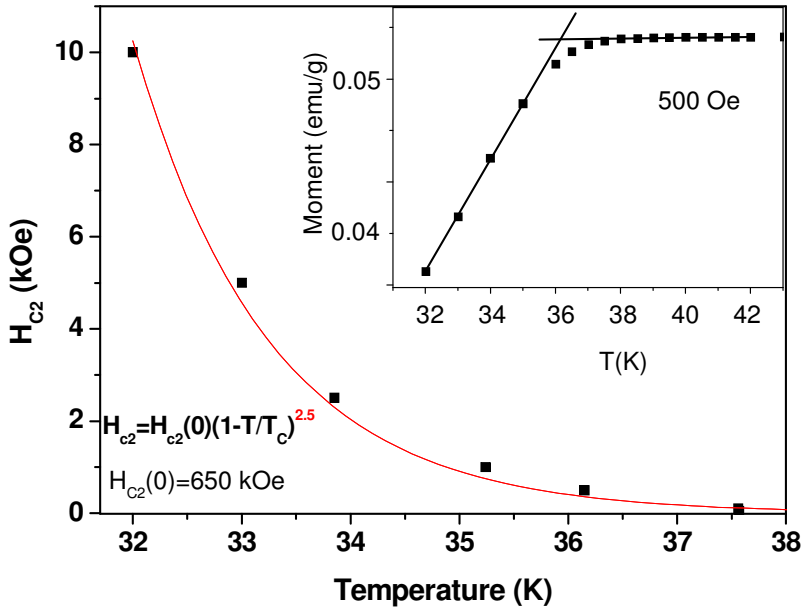

AC-S
5 K
Moment (emu/g)
Field (kOe)
0.0
0.3
0.6
0.9
1.2
0
10
20
30
40
50
M (emu/g)
H (Oe)
0.02
0.03
0.04
0
200
400
600
800
1000

Lower and Upper critical fields









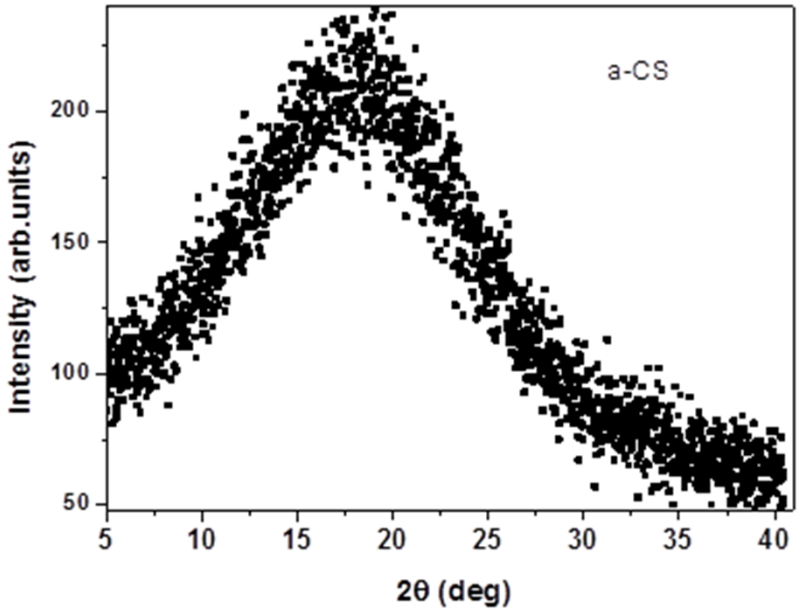
Unconventional SC state in A-C+S

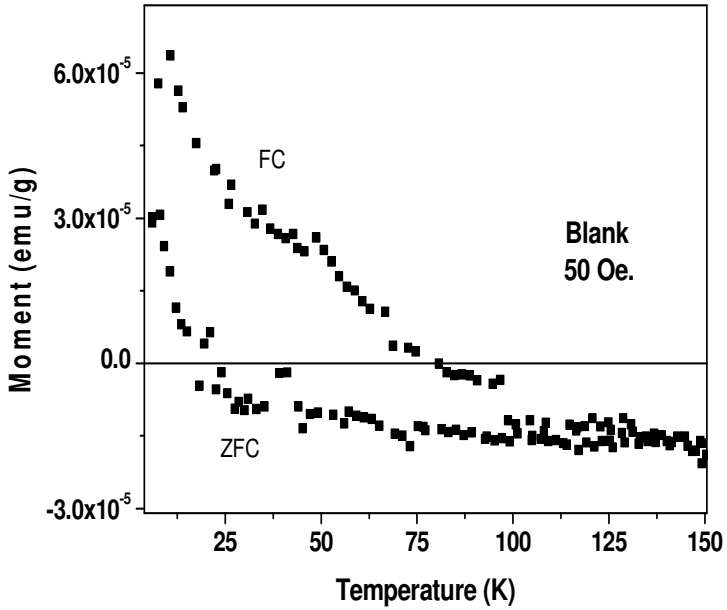
probably p-wave SC

- *Israel Felner and Yakov Kopelevich*, Phys. Rev. B **79**, 233409 (2009).

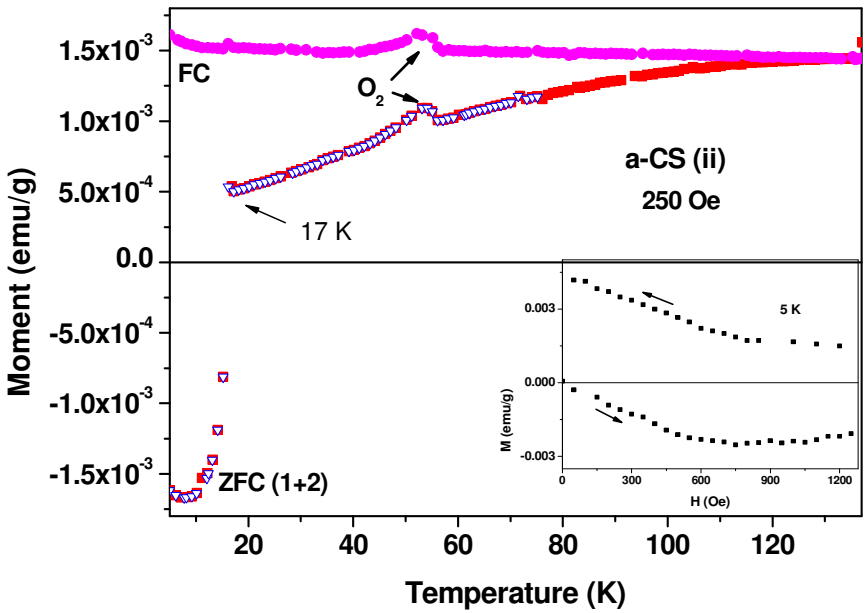
2) The fabricated a-C powder was obtained by multi-stage thermal treatment of:

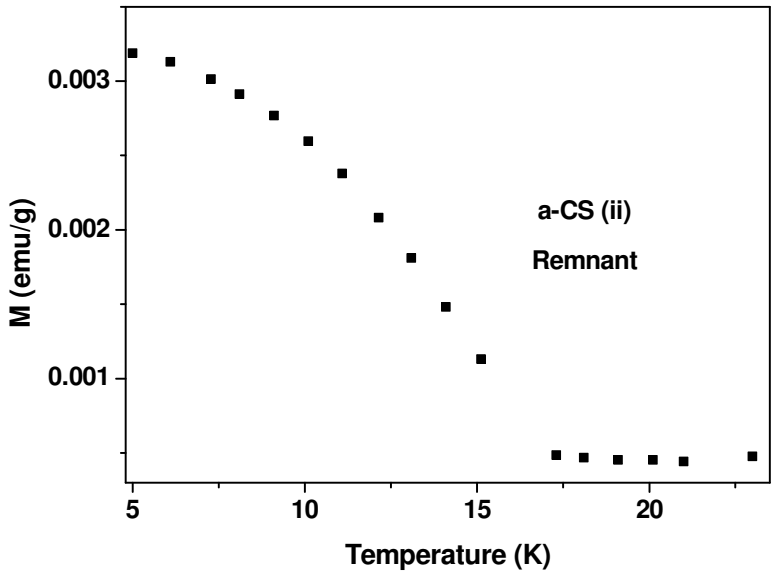
ultra pure sucrose ($C_{12}H_{22}O_{11}$) with Fe content < 3 ppm.

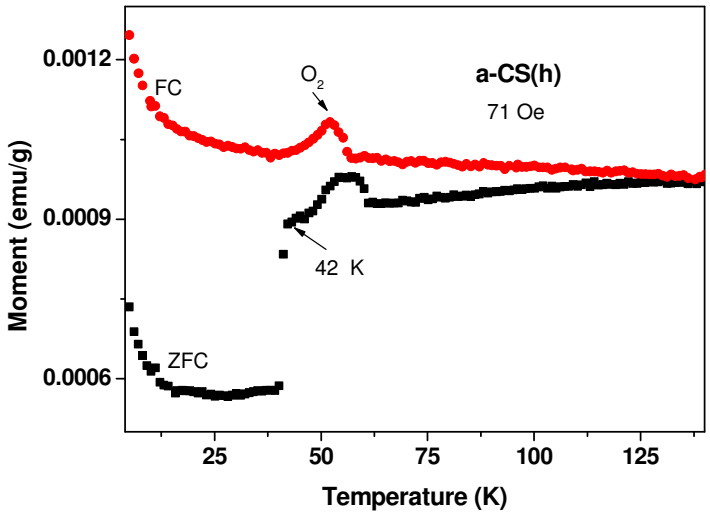




I. Felner and E. Prilutskiy J. Supercond. Nov. Magn. **25,**2547(2012)





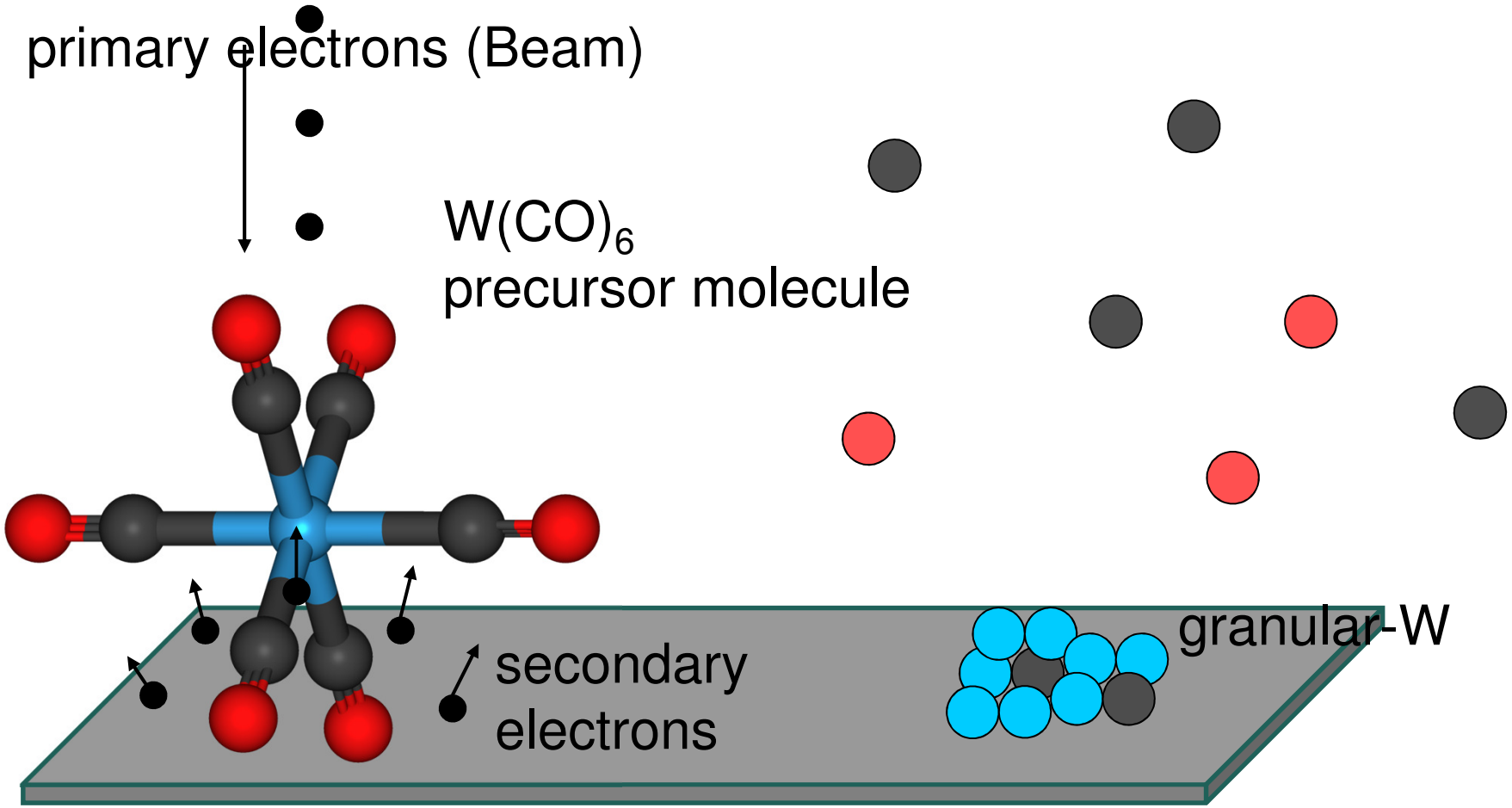


aC-S was heated at 250 C for 20 hours

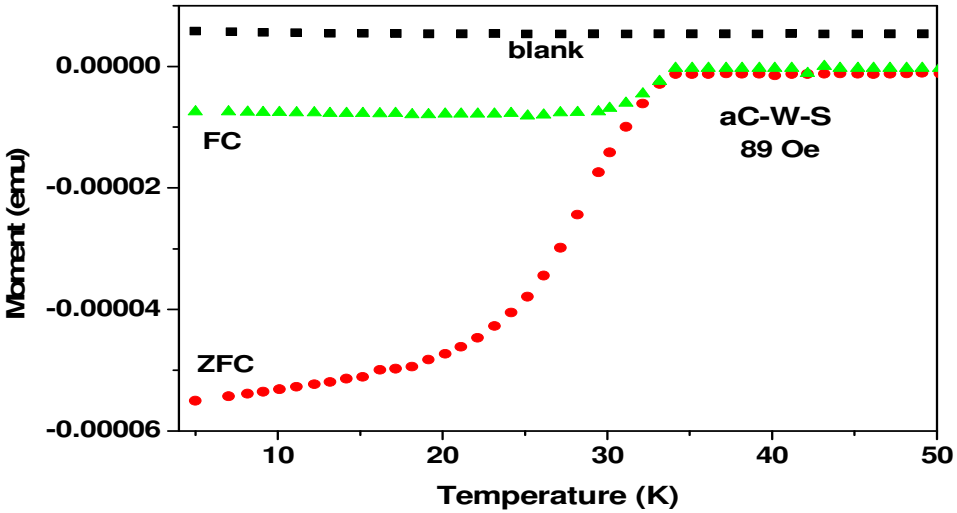
aC-S(h) was heated further at 380 °C for 3 more hours

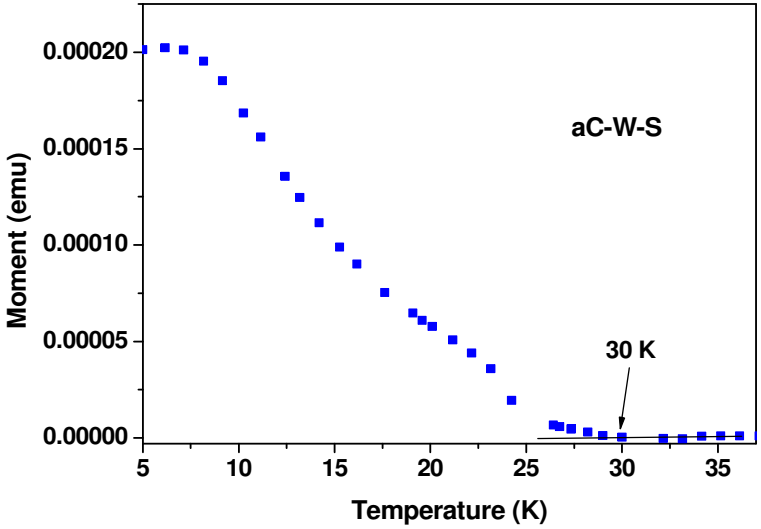
3) Superconductivity in Sulfur-Doped aC films grown by:

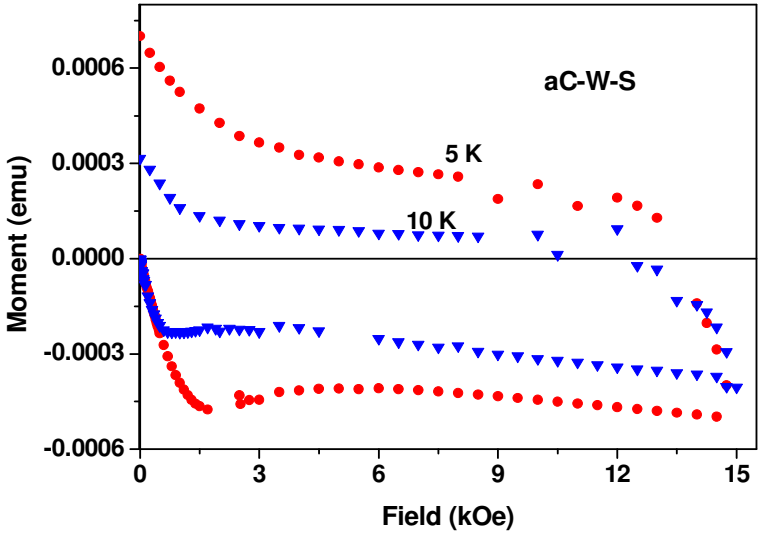
Electron Beam Induced Deposition (EBID)



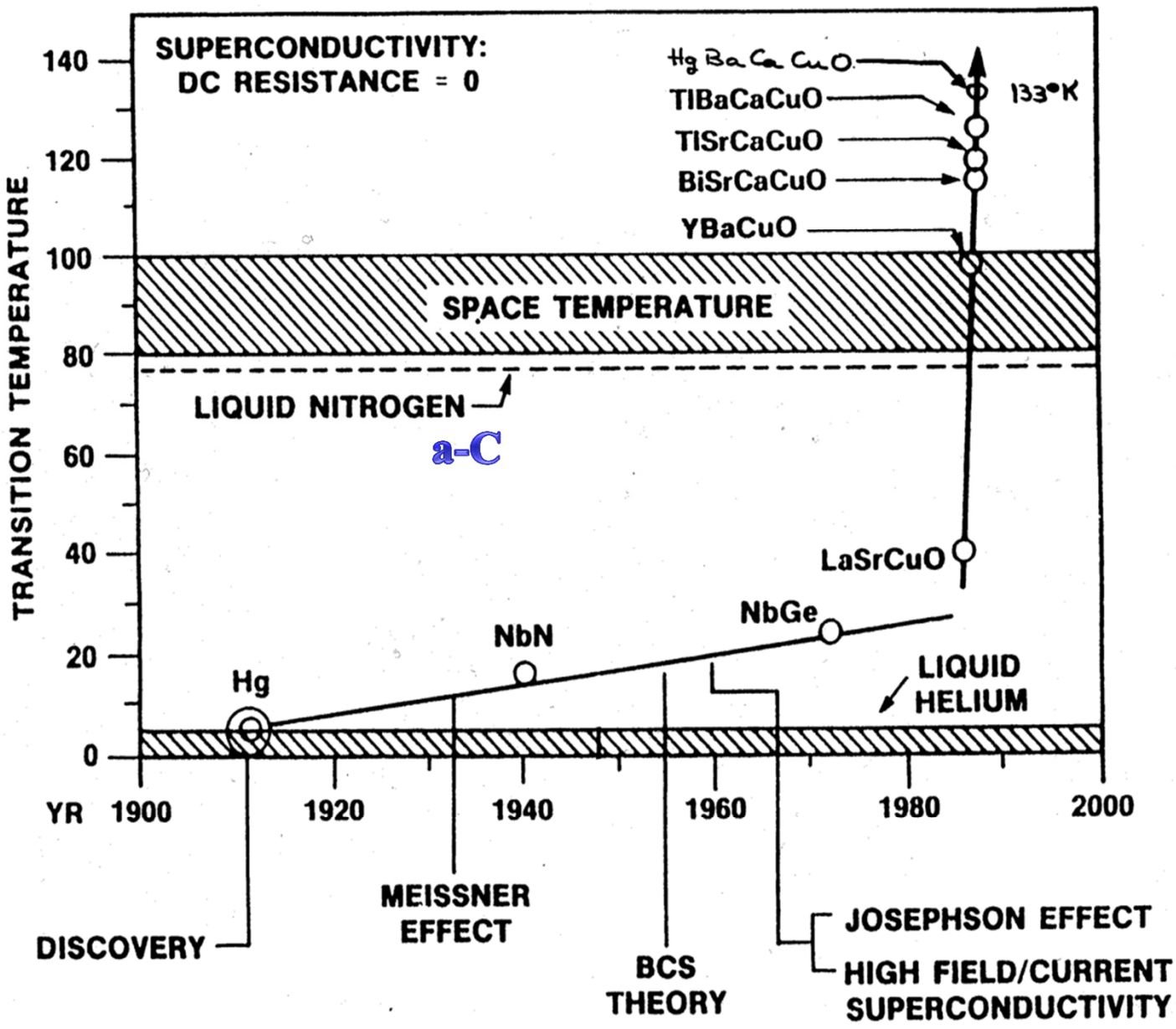
aC- films +S







- I. Felner · O.Wolf · O. Millo, J. Supercond. Nov. Magn. (2013)


SUPERCONDUCTIVITY:
DC RESISTANCE = 0
HgBaCaCuO
TlBaCaCuO
TlSrCaCuO
BiSrCaCuO
YBaCuO
133°K
SPACE TEMPERATURE
LIQUID NITROGEN
a-C
LaSrCuO
NbGe
NbN
Hg
LIQUID
HELIUM
TRANSITION TEMPERATURE
140
120
100
80
60
40
20
0
YR 1900
1920
1940
1960
1980
2000
DISCOVERY
MEISSNER
EFFECT
BCS
THEORY
JOSEPHSON EFFECT
HIGH FIELD/CURRENT
SUPERCONDUCTIVITY

P. Esquinazi et al. (Carbon, **59**, 140, 2013) reported evidence for SC in bulk highly oriented pyrolytic graphite (HOPG) samples **at room temperature**.

They found that the different internal microstructure of bulk HOPG samples led to completely different responses and suppose that SC is located at the **interfaces**.

No indication of SC was found in a sample without interfaces.

Summary of Part 1

- SC was observed in 3 different a-C sources:

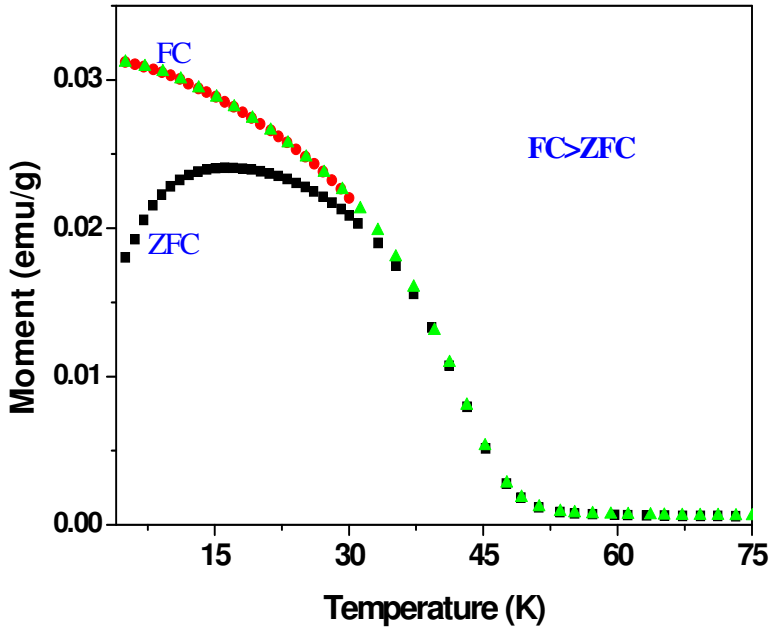
- 1) Commercial a-C and in a-C+S samples
- 2) a-C synthesized by decomposition of glucose in which sulfur was added
- 3) Thin films of a-C+S

- **Conclusions**: Traces of SC phases with T_c up to
- 65 K **definitely** exists in a-C+S based materials (although their composition is not yet known)

Part 2: Peculiar magnetic features

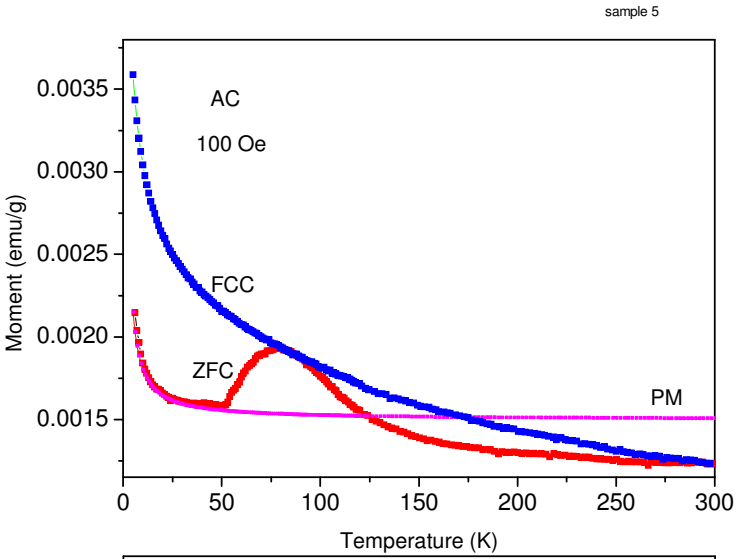
1) Pristine commercial a-C (4 samples)
and in a-C+S (heated at 400 C)

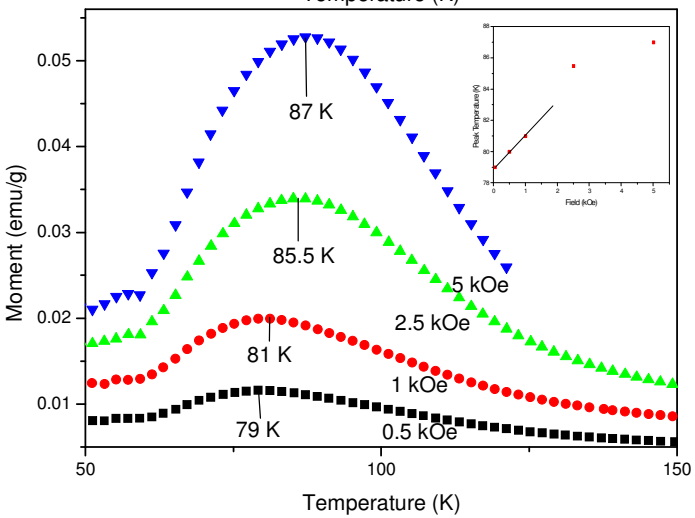
2) Fabricated a-C



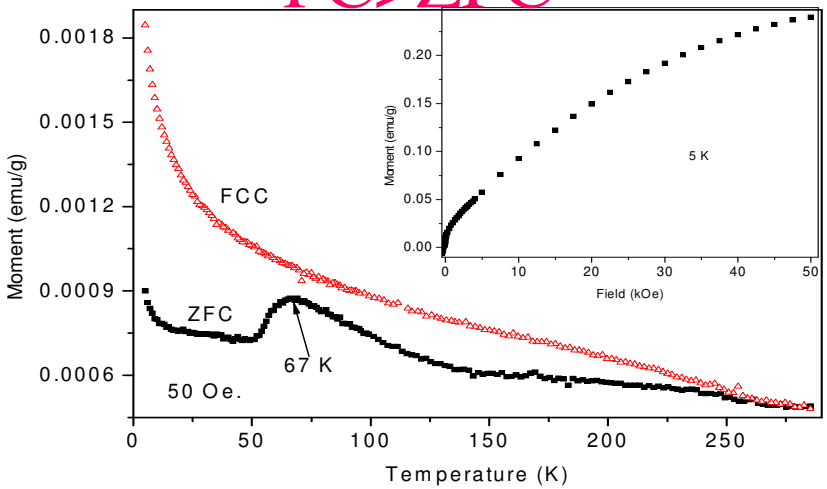
1) Commercial aC samples no. 3 and 5 are magnetic

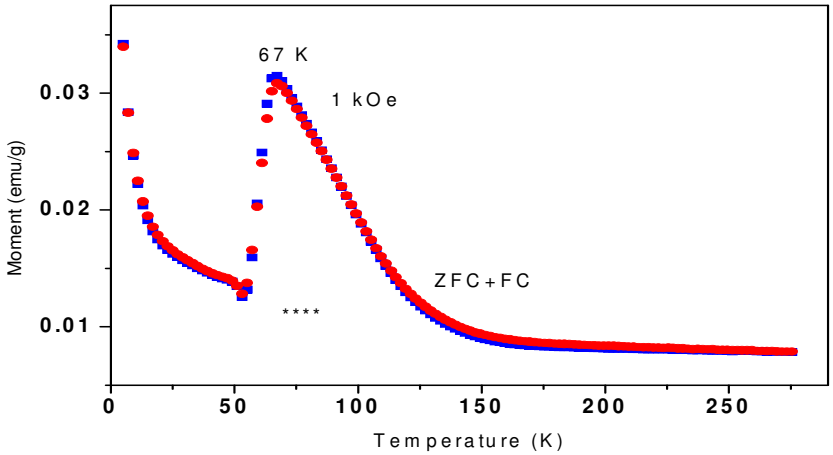
sample 5





sample 3
FC>ZFC



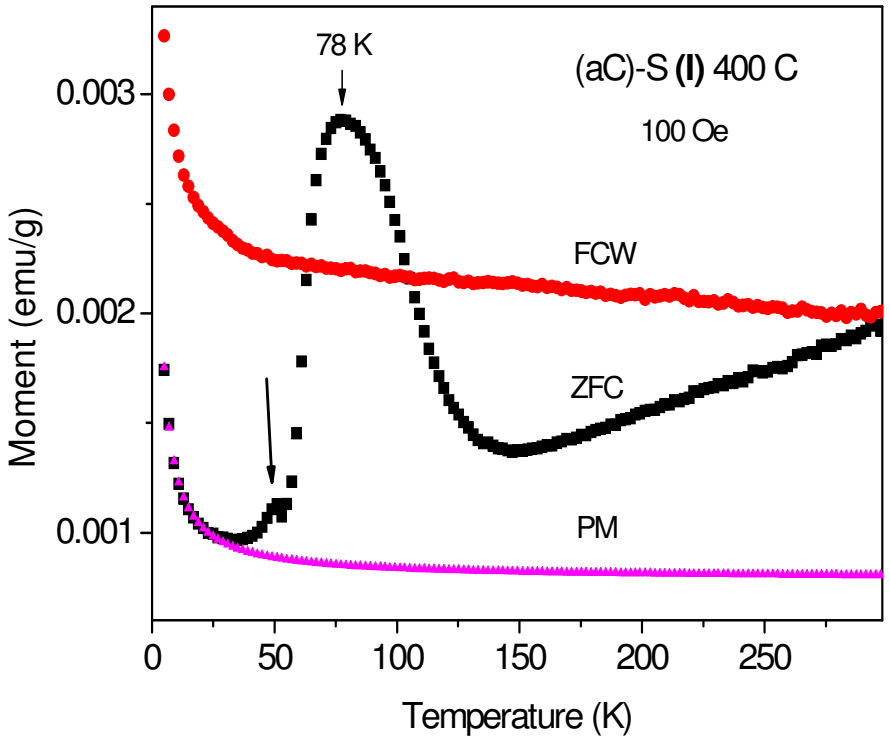


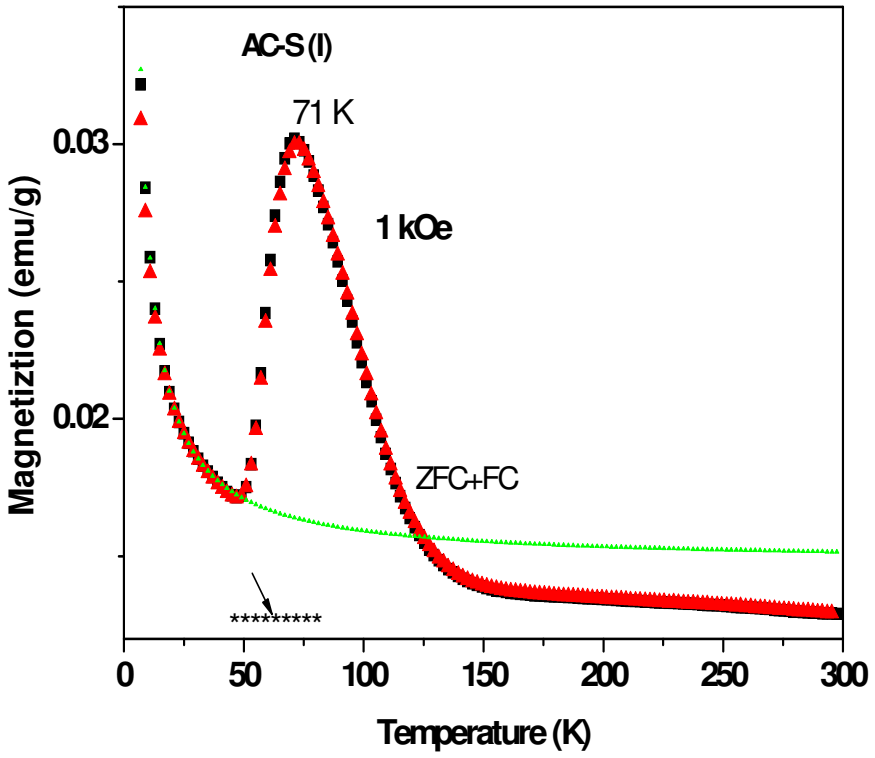
a-C+S (heated at 400 C) (3 batches)
Inhomogeneity

Samples from the same batch show significant different magnetic behavior.

Obviously, samples from different batches behave differently.

Commercial a-C+S (heated at 400 C) (batch 1 sample 1)



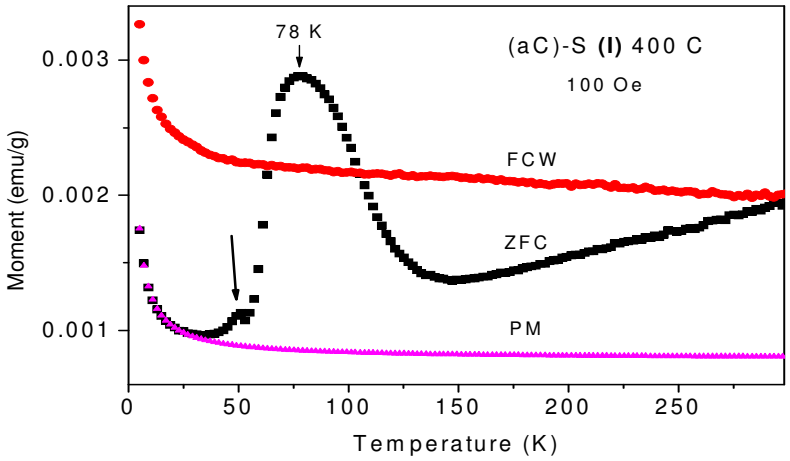


(a) ZFC>FC (at low H only) (puzzle 1)

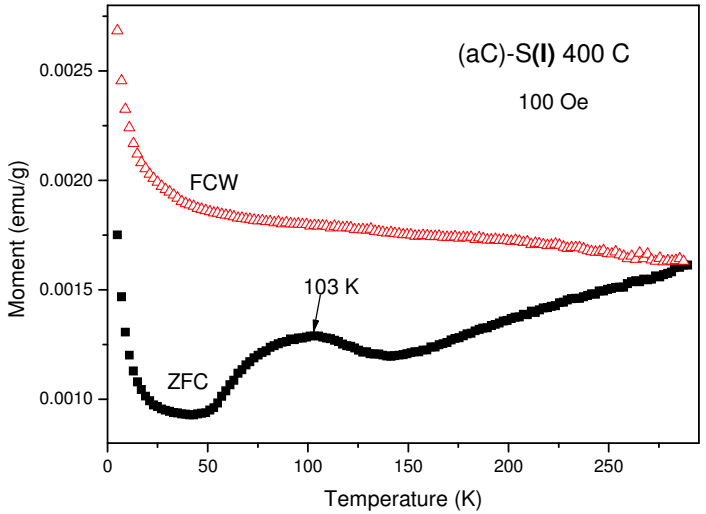
b) The peak shifts with H

Batch 1: commercial a-C+S (heated at 400 C)

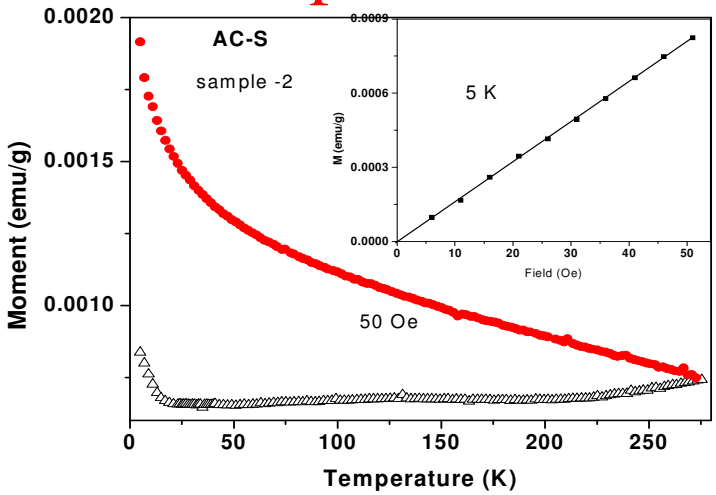
sample 1



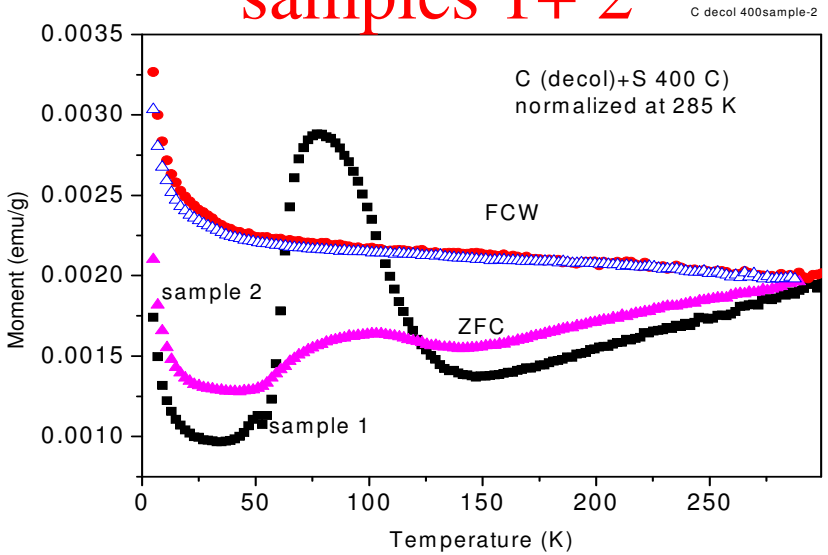
sample 2



sample 3

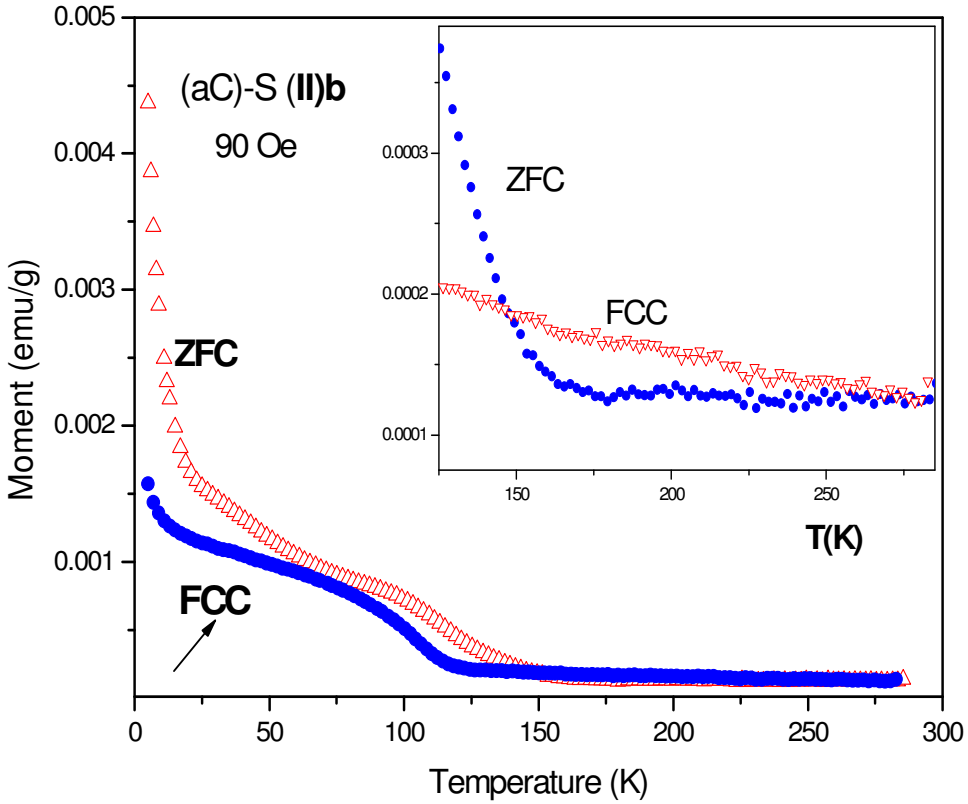


samples 1+ 2

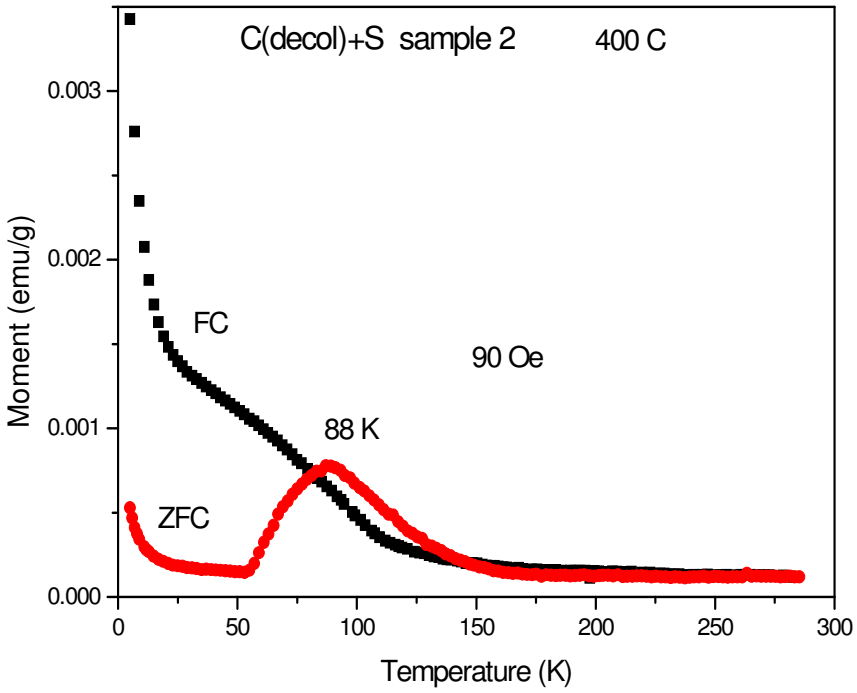


Batch 2 a-C+S (heated at 400 C)

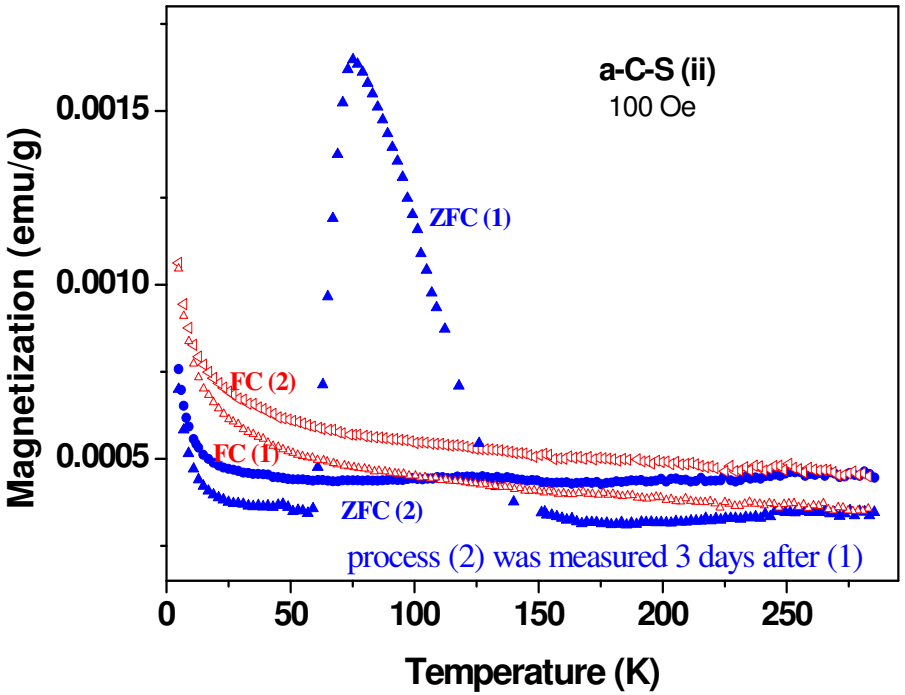
sample 1

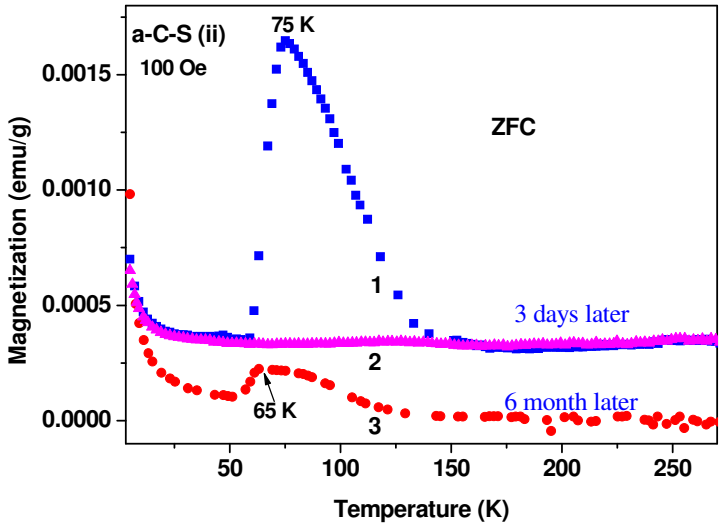


sample 2



Batch 3 sample 2

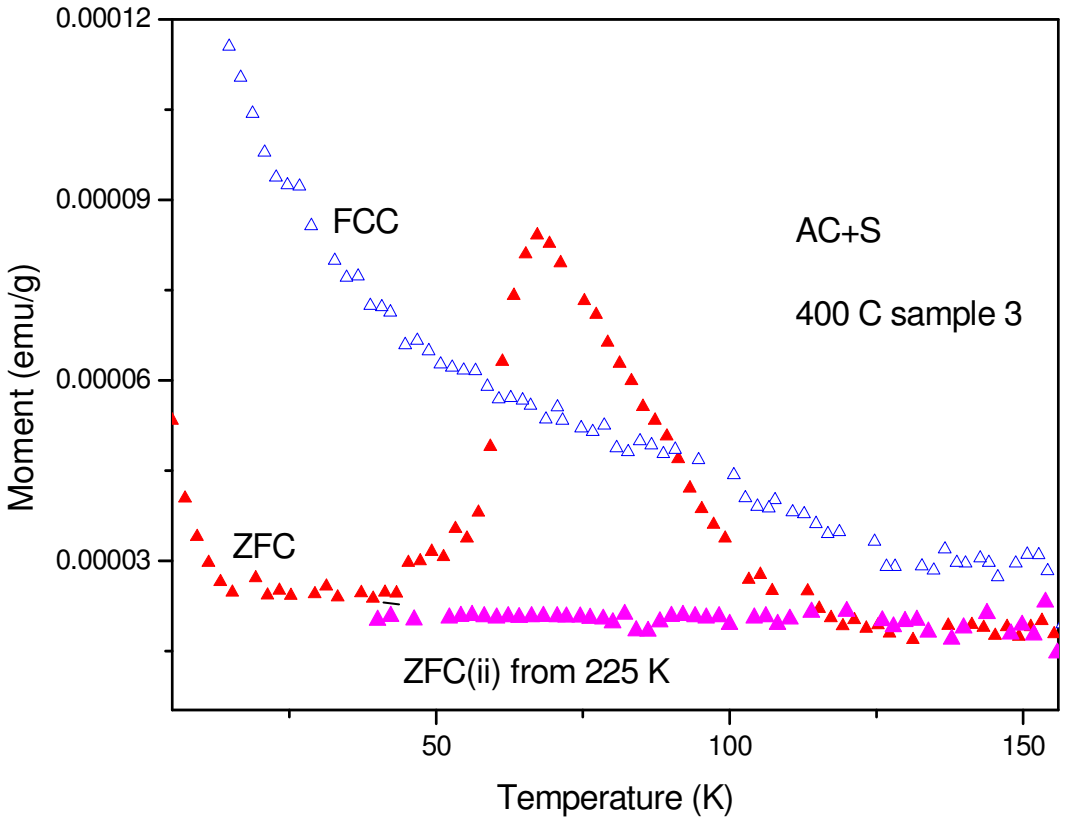




puzzle 2 the ZFC peak disappears in the second run

Puzzle 3 the ZFC peak **reappears** after 6 months

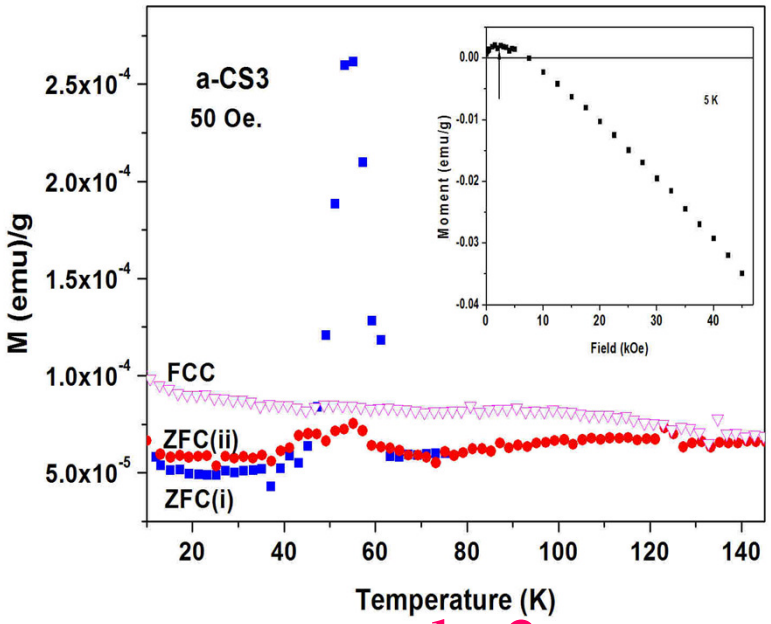
Batch 3 sample 3



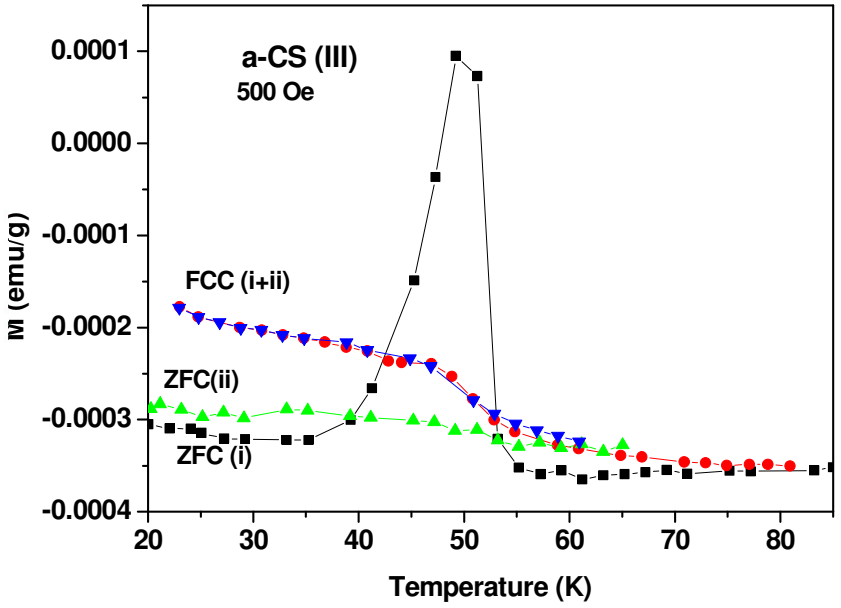
Puzzle 2

1) ZFC up to 225 K **field off**
2) ZFC (ii) up to 225 K
3) **FCC** down to 5 K

2) synthesized **a-C (sucrose)** samples



sample 2

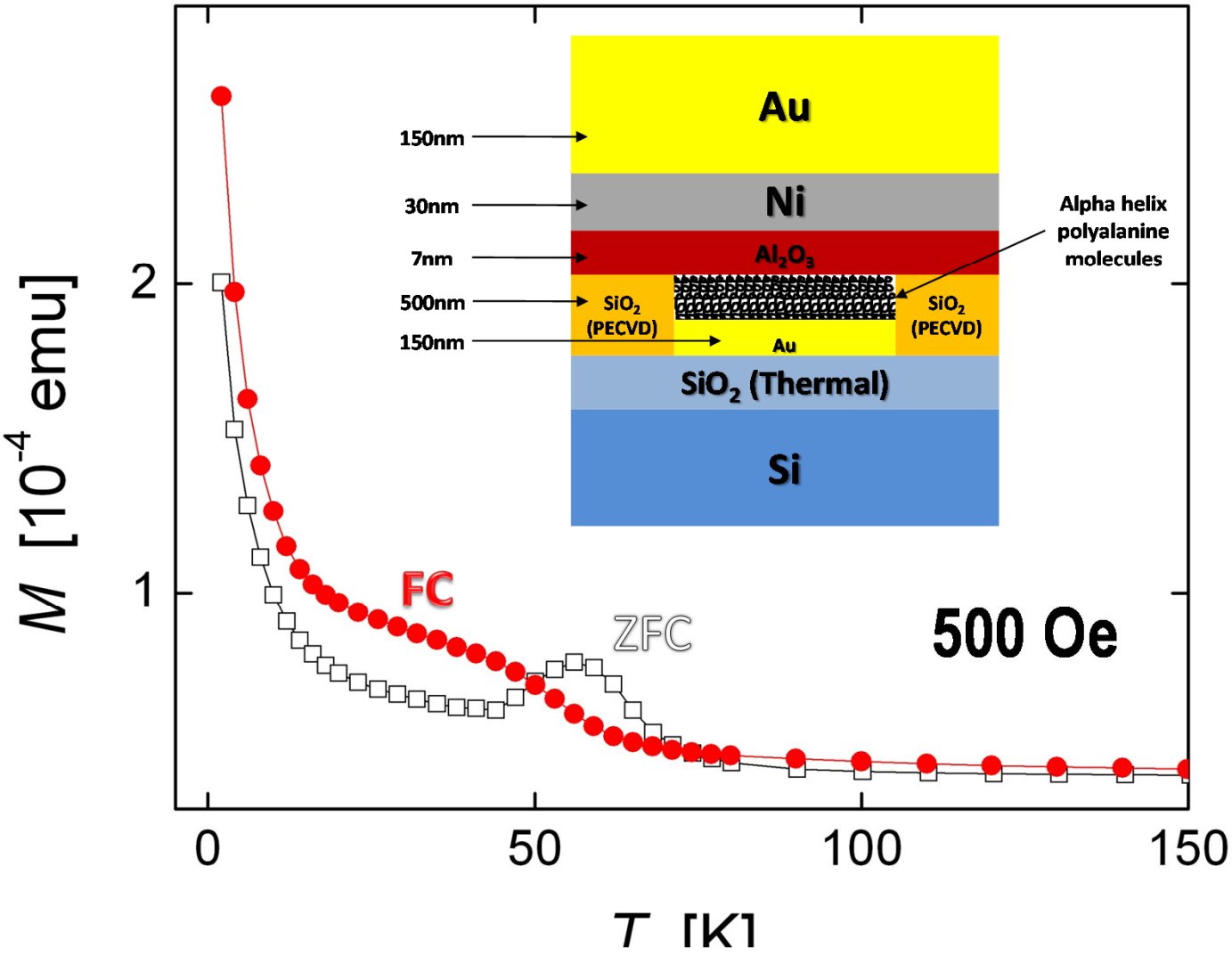


sample 3

The peak in the ZFC branch (if exists) is observable in the first run only (**puzzle 2**).

As a result, the FC branch penetrates inside the ZFC branch **(puzzle 1)**

O.Ben Dor et al. *Nature Communications* **4,** 2256 (2013).



The origin of the peak

- structural disorder (curvature)
- presence of a foreign atom such as sulfur

The peak's disappearance

- **As a hand waiving**: two-state system separated by an **energy barrier**, (such as a double-well potential) with a finite probability of finding the system in one of the two wells

Summary part 2

- At low H the peak in the ZFC branch is observable **in the first run only** (puzzle 2).
  As a result, the FC branch penetrates inside the ZFC branch (Puzzle 1)

- After half a year the ZFC peak reappears

- The main question remains as the origin of the peak in the ZFC branch ???

- Thanks for your kind attention

Questions

- 1) Did you manage to measure the resistivity ???
- 2) Does the peak disappear in ac studies??

כן ולא

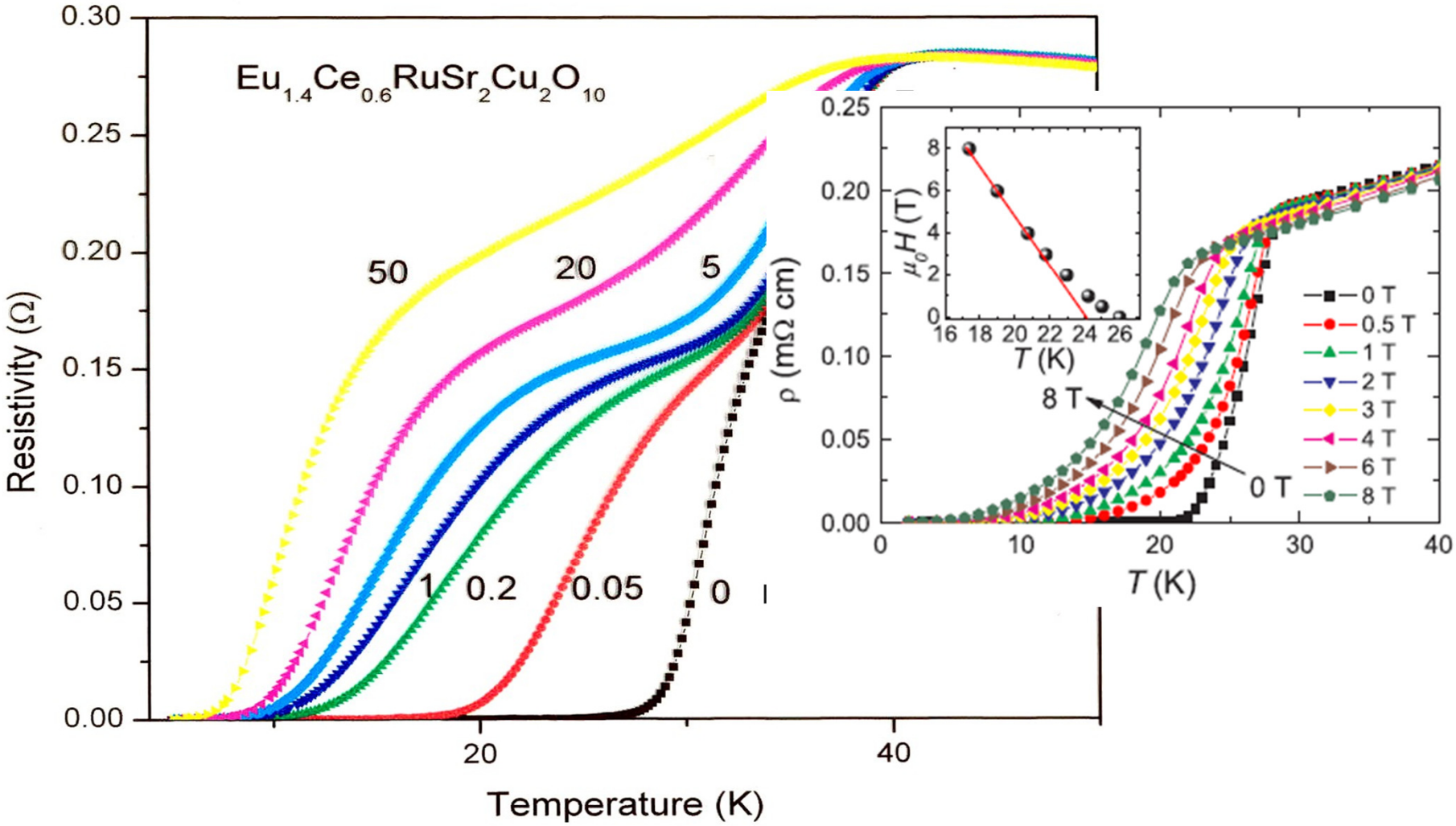
- Why don't you see the Verway transition in your materials??

diamagnetism

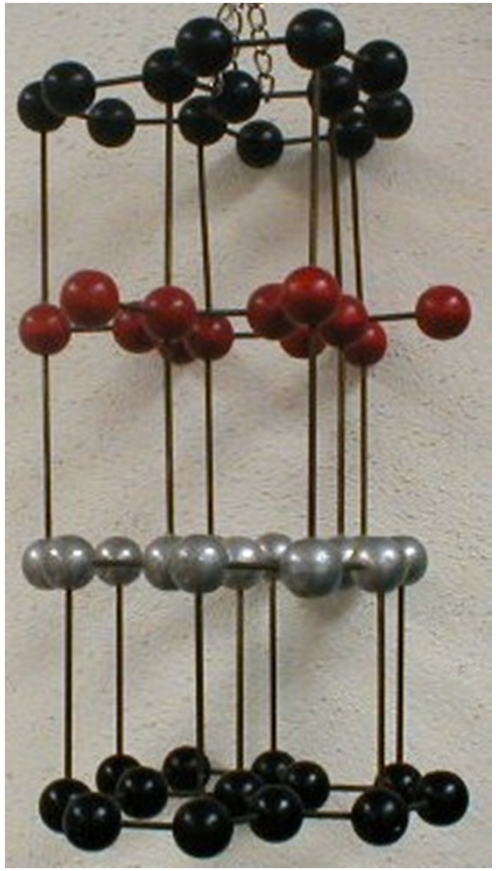


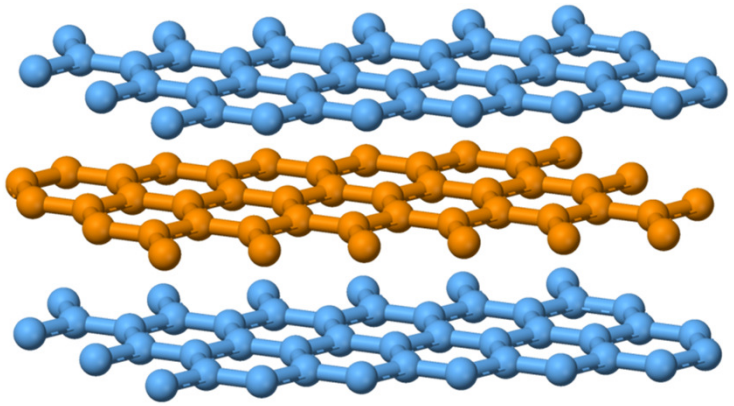


- Ferromagnetism or any magnetic order is typically the property of transition and rare-earth metals, alloys and intermetalic compounds, with unpaired electrons in unfilled atomic shells.
- carbon atoms show very strong tendency to pair up their outer-shell electrons in covalent bonds.
- graphite in which sp^2 hybridization forms planar sheets in a two layer hexagonal stacking.
- diamond in which sp^3 carbons (band gap E_g=5.4 eV) form a three-dimensional lattice of cubic symmetry

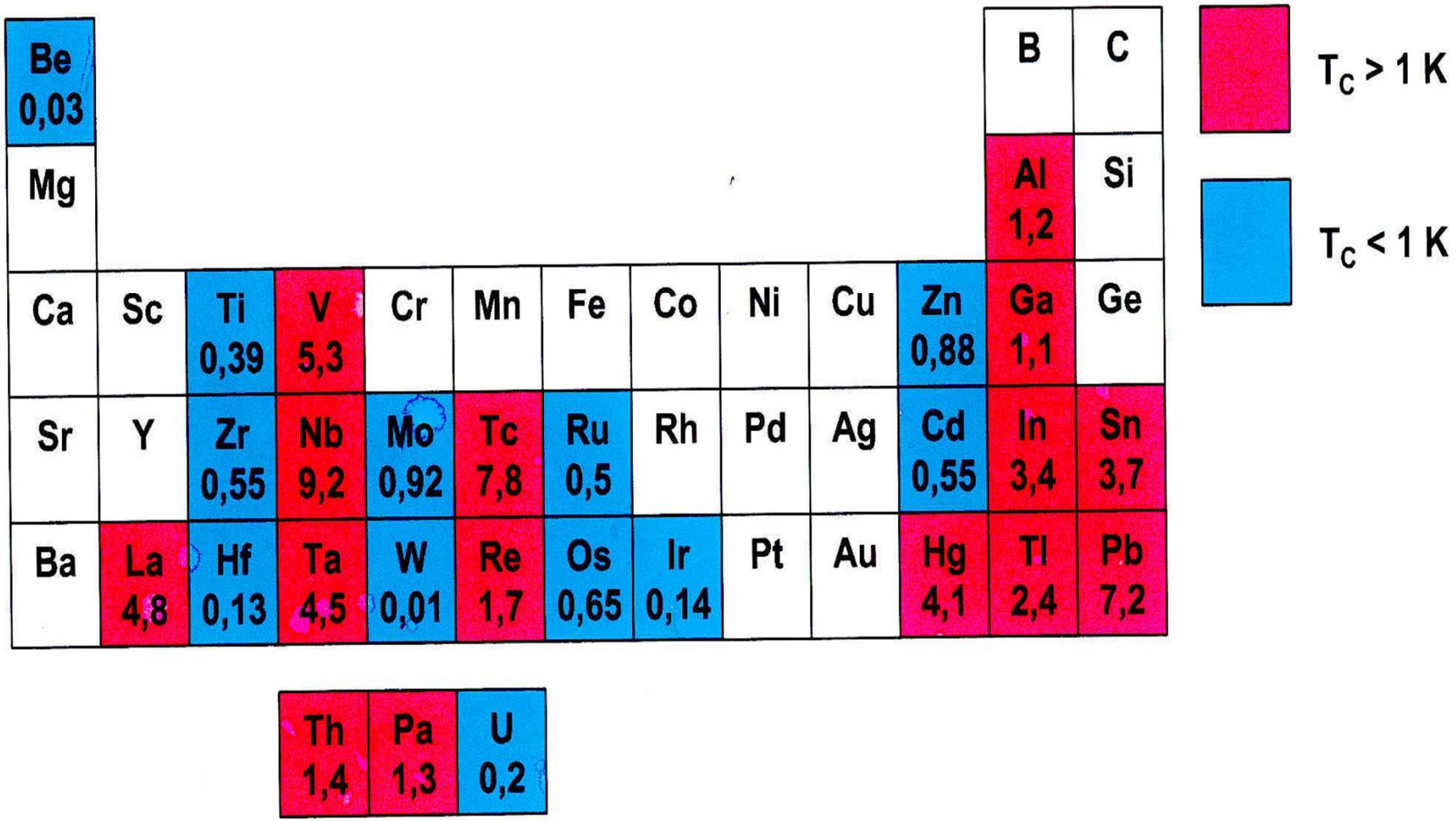

Eu1.4Ce0.6RuSr2Cu2O10
Resistivity (Ω)
Temperature (K)
0.30
0.25
0.20
0.15
0.10
0.05
0.00
20
40
50
20
5
1
0.2
0.05
0
ρ (mΩ cm)
μ0H (T)
T (K)
8 T
0 T
0 T
0.5 T
1 T
2 T
3 T
4 T
6 T
8 T

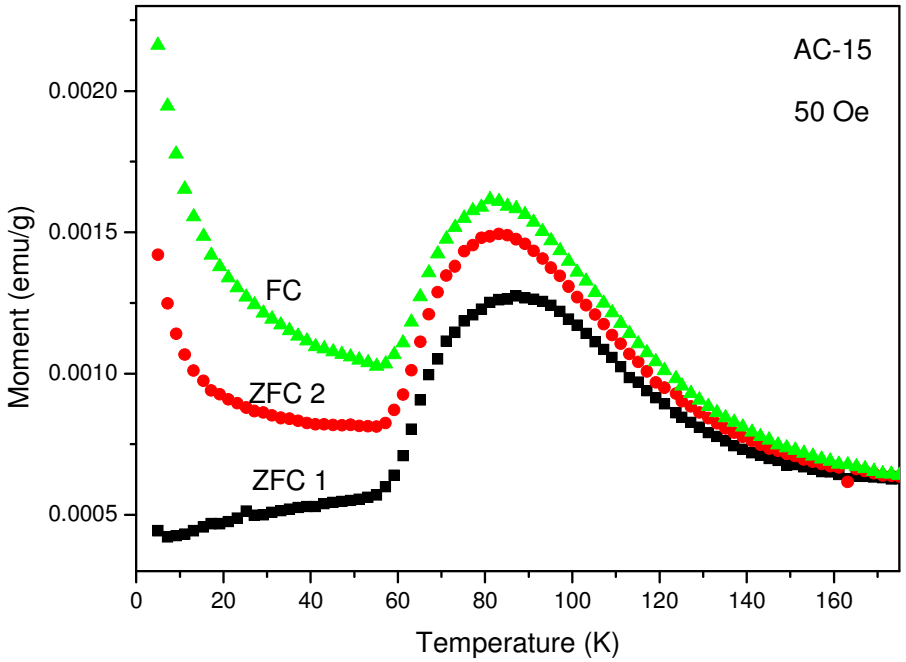
Graphite





Superconductors
Superconducting Elements




AC-15
50 Oe
FC
ZFC 2
ZFC 1
Moment (emu/g)
Temperature (K)
0.0020
0.0015
0.0010
0.0005
0
20
40
60
80
100
120
140
160

Ferromagnetic- and Superconducting-Like Behavior of Graphite

Y. Kopelevich,[1,*] P. Esquinazi,[1] J. H. S. Torres,[*] and S. Moehlecke[2]

JLTP- 119.691 (2000)

HPOG

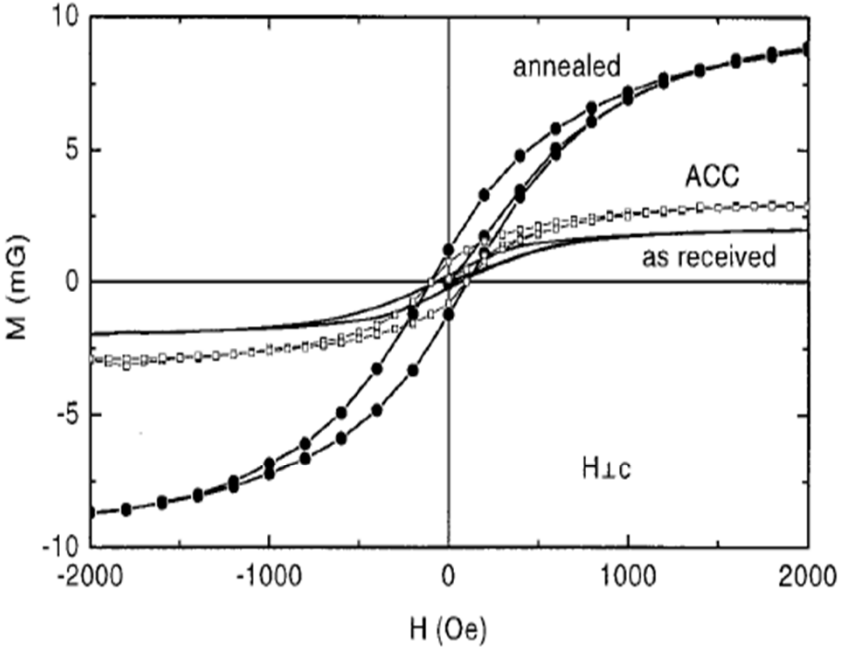


Fig. 2. Ferromagnetic-like $M(H \perp c)$ hysteresis loop measured at $T = 300$ K in the HOPG-2 sample ($V_3 = 2.45 \times 2.15 \times 1.9$ mm^3) before annealing (continuous line) at 800 K for 2 hours, and $M(H \perp c)$ measured at $T = 350$ K after annealing (●). (□): $M(H \perp c)$ measured at $T = 300$ K on as-received sample from Advanced Ceramic Corporation (ACC) (the sample size is $3.6 \times 3.5 \times 1$ mm^3).

Different **HPOG** volumes $V_1 > V_2$

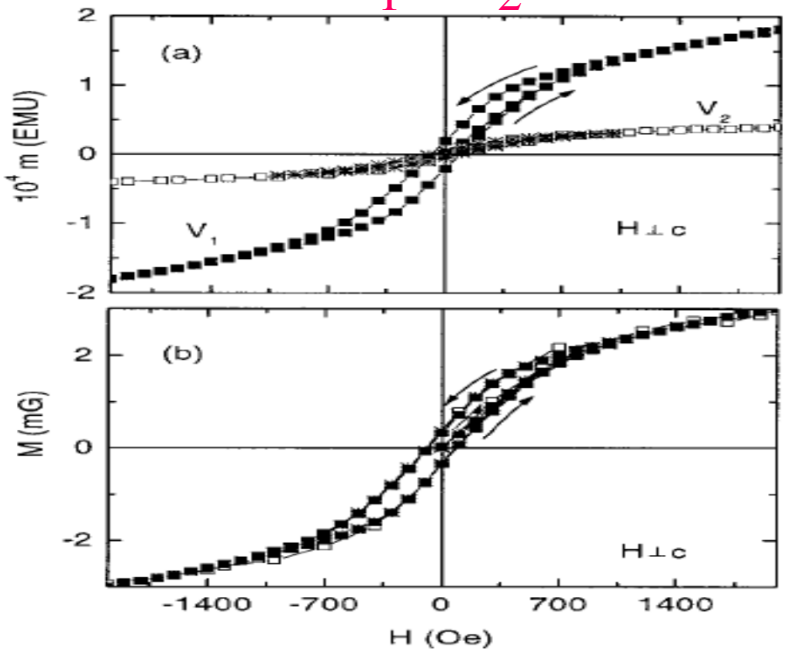
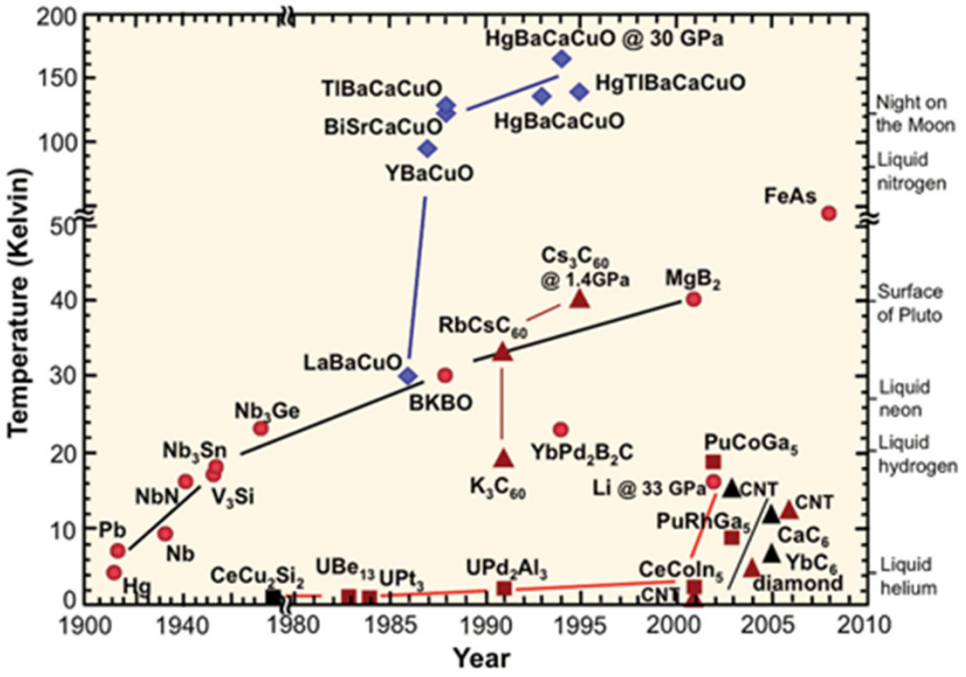


Fig. 1. (a) Magnetic moment $m(H)$ hysteresis loops measured in HOPG-2 samples with two different volumes ($V_1/V_2 \simeq 4.4$) at $T = 100$ K and magnetic field applied parallel to the graphite basal planes ($H \perp c$). We show for sample V_2 the hysteresis loops measured with two different field cycles (□, ∗). (b) Magnetization $M(H) = m(H)/V$ data from (a) demonstrating that m(H) is proportional to the sample volume.


Temperature (Kelvin)
Year
HgBaCaCuO @ 30 GPa
TlBaCaCuO
HgTlBaCaCuO
BiSrCaCuO
HgBaCaCuO
YBaCuO
FeAs
Cs3C60 @ 1.4GPa
MgB2
RbCsC60
LaBaCuO
BKBO
Nb3Ge
Nb3Sn
YbPd2B2C
PuCoGa5
K3C60
Li @ 33 GPa
CNT
NbN
V3Si
PuRhGa5
CaC6
Pb
Nb
YbC6
diamond
Hg
CeCu2Si2
UBe13
UPt3
UPd2Al3
CeCoIn5
Night on the Moon
Liquid nitrogen
Surface of Pluto
Liquid neon
Liquid hydrogen
Liquid helium

PHYSICAL REVIEW B 74, 214418 (2006)

Ferromagnetic behavior of carbon nanospheres encapsulating silver nanoparticles

R. Caudillo,[1,*] X. Gao,[1] R. Escudero,[2] M. José-Yacaman,[1,3] and J. B. Goodenough[1]

Pressed sample

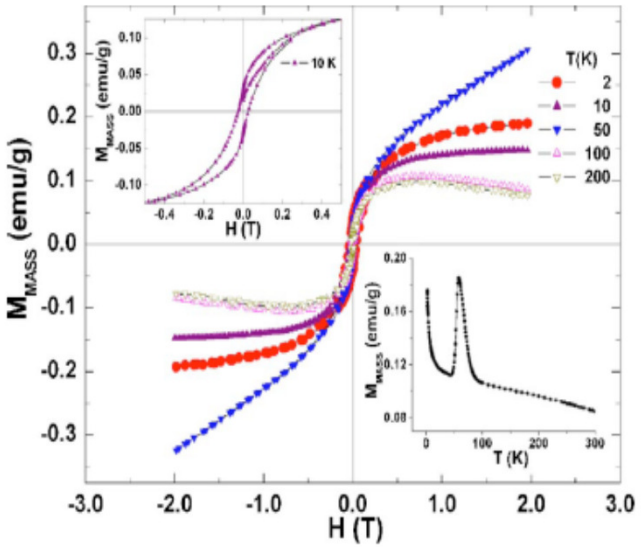


FIG. 9. (Color online) Selected $M_{mass}(H)$ curves for a ZFC powder sample. Upper left inset, close up of $M_{mass}(H)$ curve at 10 K clearly showing ferromagnetic hysteresis. Lower right inset, corresponding $M_{mass}(T)$ ZFC curve.

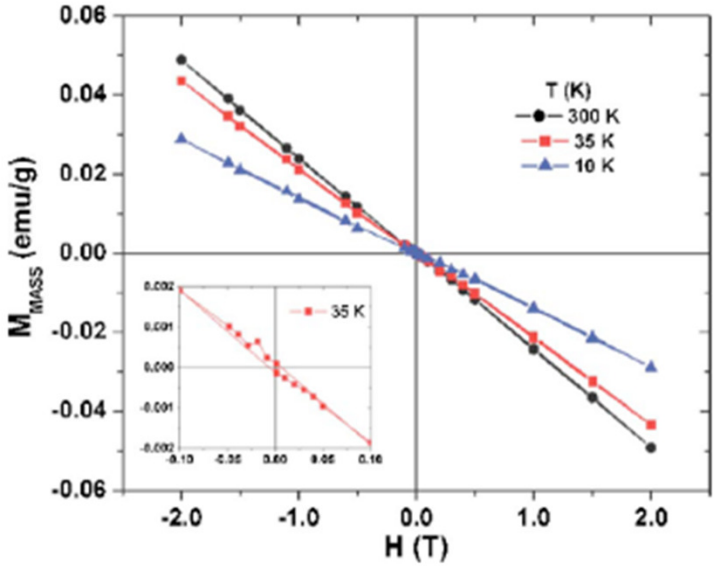
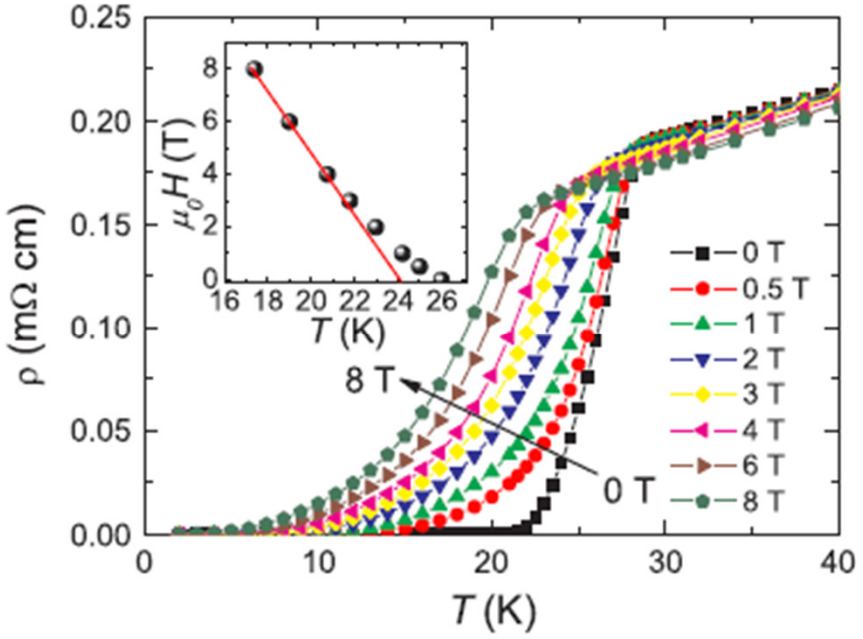
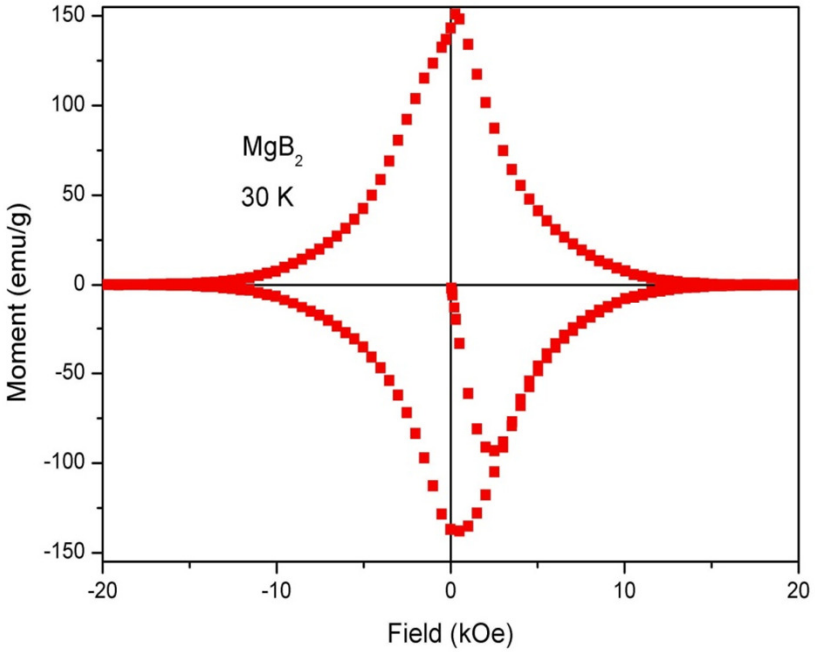


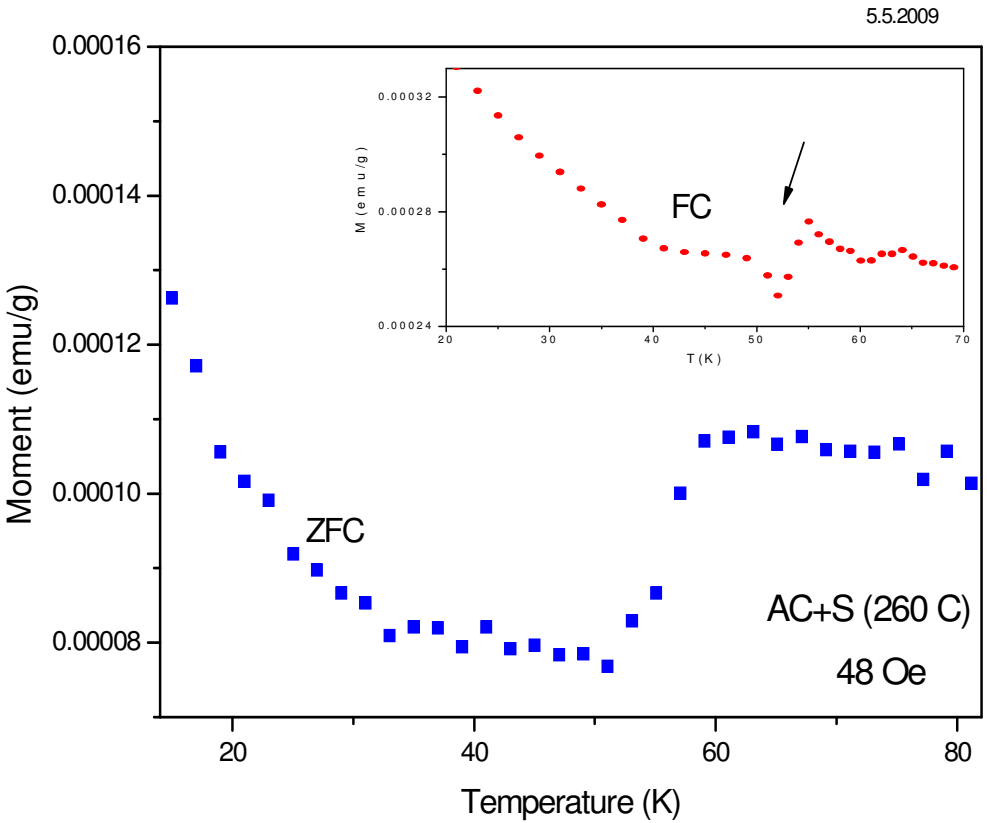
FIG. 11. (Color online) Selected $M_{mass}(H)$ curves for a pressed sample at 10 K, 35 K, and 300 K, clearly showing the absence of ferromagnetic hysteresis and complete transition to diamagnetic behavior in the pressed samples. Inset, magnified view of $M_{mass}(H)$ curve at 35 K showing the diamagnetic behavior at low fields.

The magnetic field effect

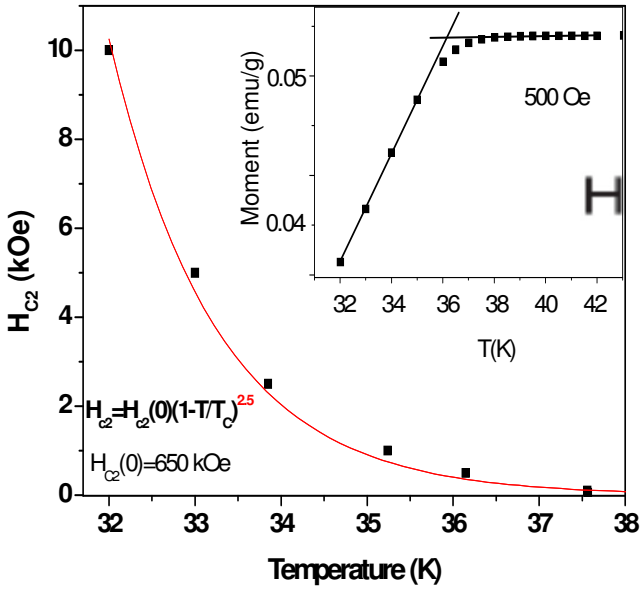




The second transition



Qi. Li et al. PRL 98, 187002 (2007)



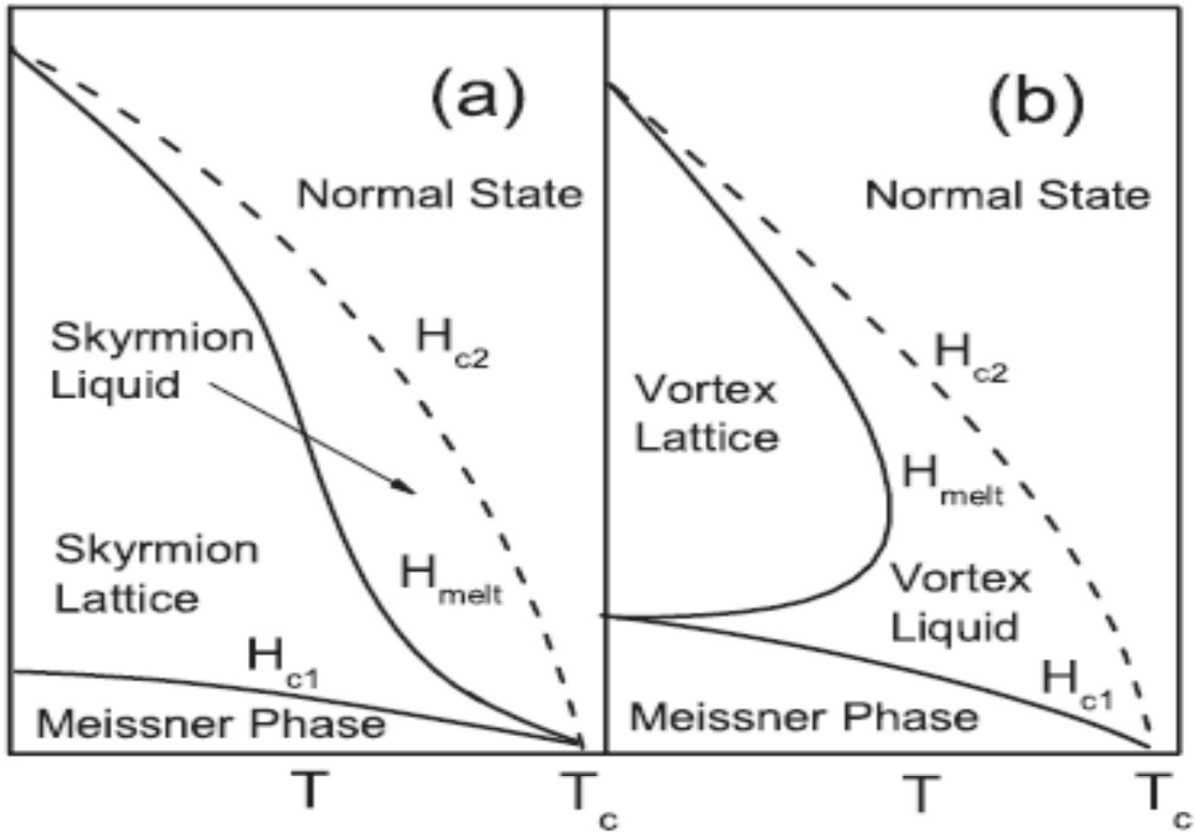
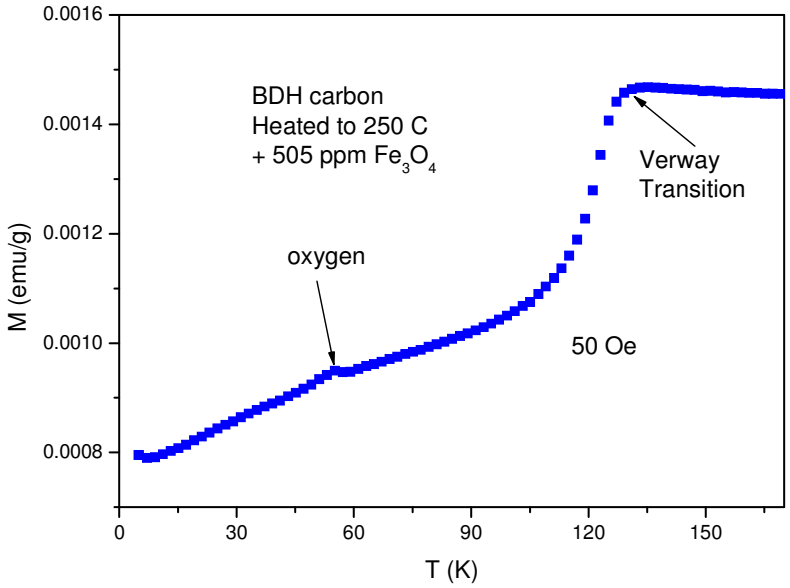
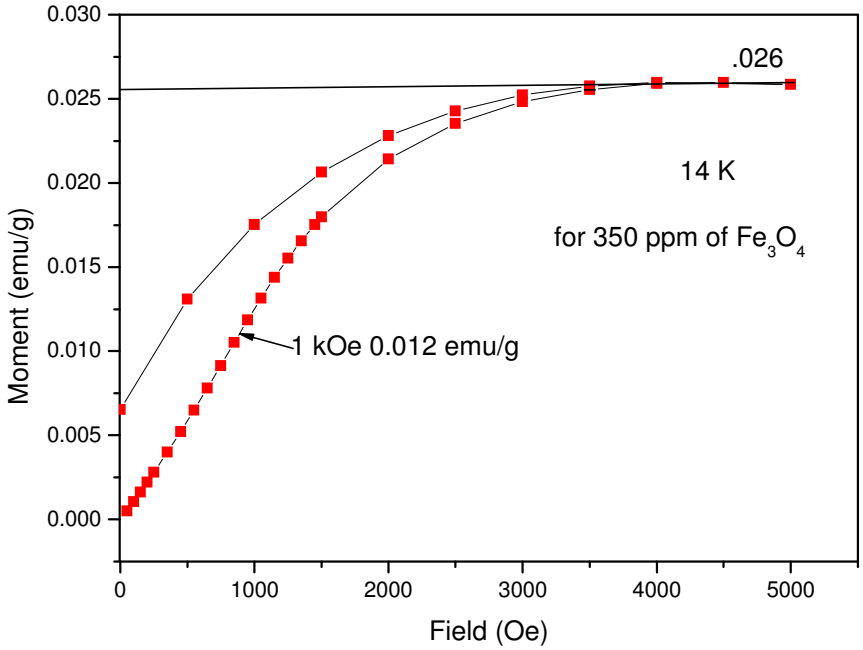


FIG. 1. (a) External field (H) vs temperature (T) phase diagram for Skyrmion flux lattices. There is a direct transition from the Skyrmion flux lattice to the Meissner phase. The theory predicts the shape of the melting curve only close to T_c; the rest of the curve is an educated guess. (b) Same as (a) for vortex flux lattices. The vortex flux lattice always melts before H reaches H_{c1}.

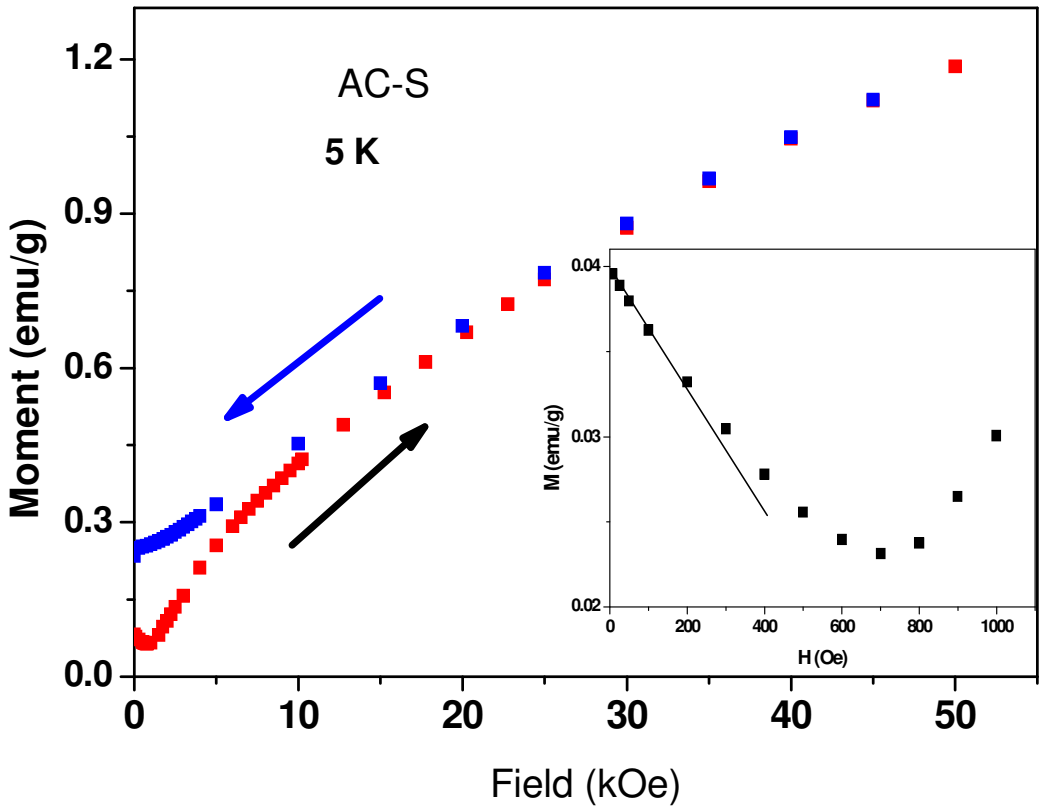
Controlled experiment C+ 500 ppm of magnetite



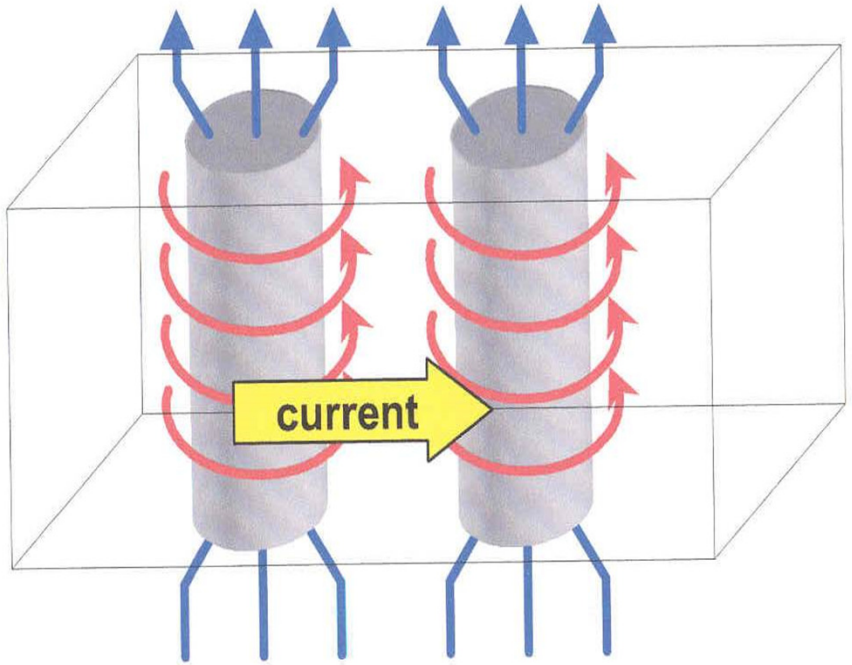


The remannet at 5 K is due to the magnetic phase Skyrmion flux(SkF)

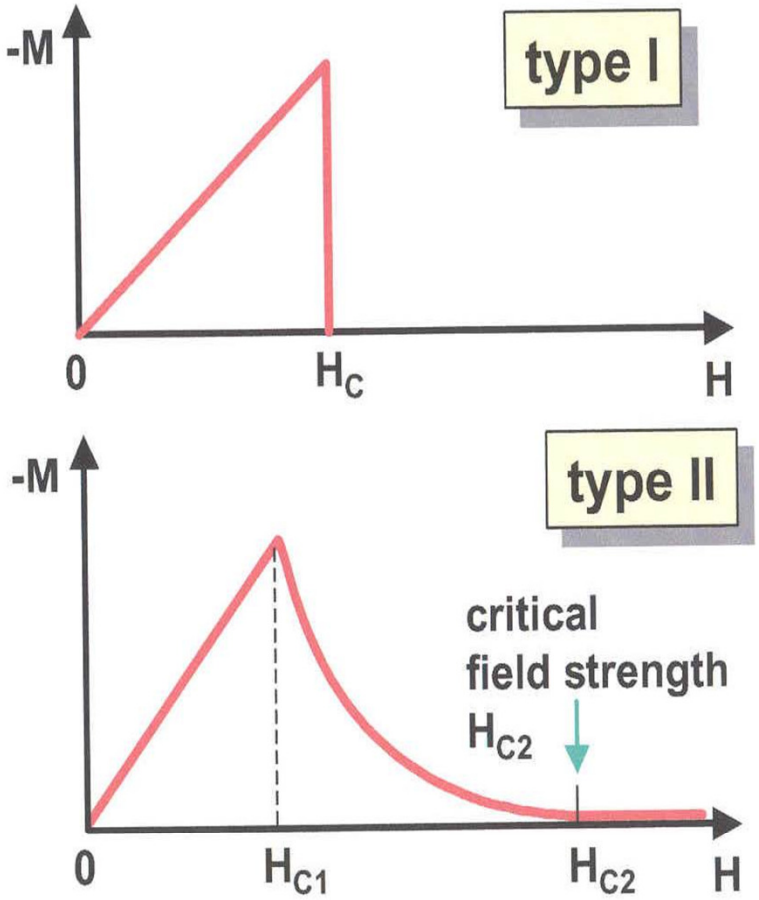
FM Griffiths phase coexists with SkF



Superconductors
Type II Superconductors

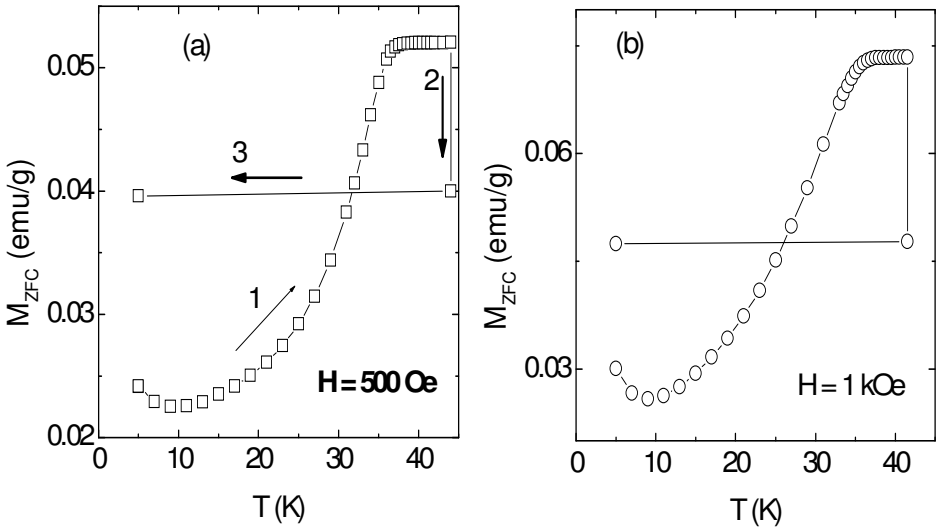


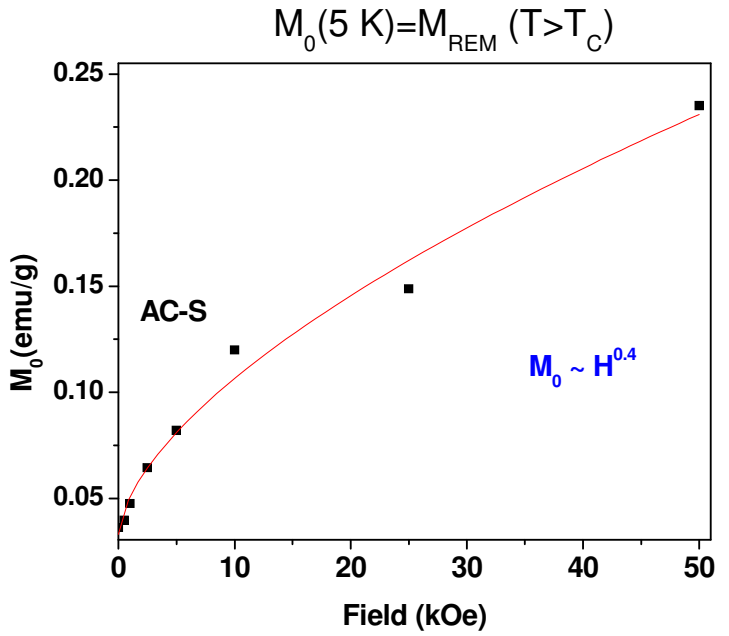
Lorentz force
magn. induction

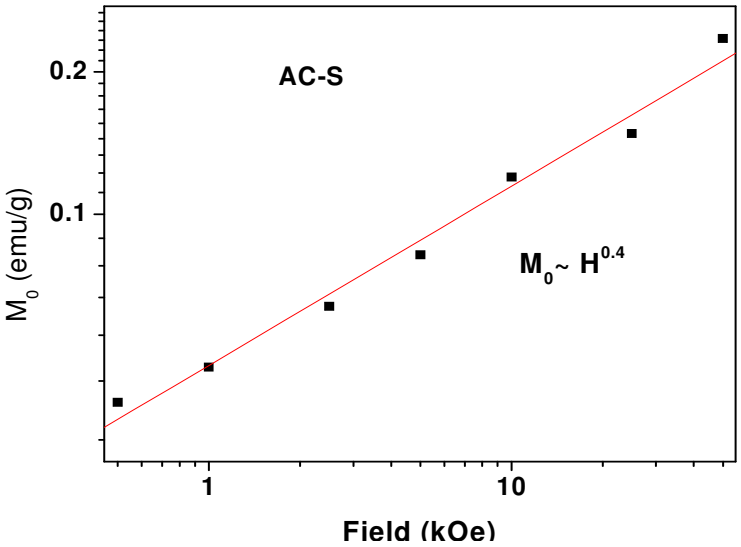


$H < H_{C1}$: Total exclusion of a magnetic field
$H_{C1} \leq H \leq H_{C2}$: magnetic field in normal conducting areas

Magnetic Griffiths phase







From a classical point of view, *every superconductor exhibits perfect diamagnetism*, i.e. $\mathrm{B} = 0$ inside the superconductor, as shown in Fig. 2.2b. In fact, as we already know, the magnetic field penetrates into the superconductor within a very thin surface layer having the thickness of the order of λ_L. To cancel B, a superconductor creates a *dc* current on the surface, which gives rise to a magnetization M, so that in the interior of the superconductor $4\pi\mathrm{M} + \mathbf{H} = 0$. Since the resistivity of the superconductor is zero, this surface current does not dissipate energy.

If the magnetic field was applied to a superconductor at $T > T_c$, and it is then cooled down to $T < T_c$, in this case, the field will remain inside the superconductor until it will be warmed up again through T_c. This "frozen" magnetic field will remain inside the superconductor independently of the presence of the external magnetic field.